

1 **The Formation of Gullies on Mars Today**

2

3 Colin M. Dundas<sup>a</sup> \*

4 Alfred S. McEwen<sup>b</sup>

5 Serina Diniega<sup>c</sup>

6 Candice J. Hansen<sup>d</sup>

7 Shane Byrne<sup>b</sup>

8 Jim N. McElwaine<sup>e, f</sup>

9

10

11 <sup>a</sup>Astrogeology Science Center, U.S. Geological Survey, 2255 N. Gemini Dr., Flagstaff,

12 AZ 86001, USA ([cdundas@usgs.gov](mailto:cdundas@usgs.gov)).

13 <sup>b</sup>Lunar and Planetary Laboratory, The University of Arizona, Tucson, AZ 85721, USA.

14 <sup>c</sup>Jet Propulsion Laboratory, California Institute of Technology, Pasadena, CA 91109,

15 USA.

16 <sup>d</sup>Planetary Science Institute, St. George, UT 84770, USA.

17 <sup>e</sup>Planetary Science Institute, 1700 E. Fort Lowell, Tucson, AZ 85719, USA.

18 <sup>f</sup>Durham University, Department of Earth Sciences, Durham, UK.

19

20

21 \*Corresponding author.

22

23

24 **Abstract**

25           A decade of high-resolution monitoring has revealed extensive activity in fresh  
26 Martian gullies. Flows within the gullies are diverse: they can be relatively light, neutral,  
27 or dark, colorful or bland, and range from superficial deposits to 10-meter-scale  
28 topographic changes. We observed erosion and transport of material within gullies, new  
29 terraces, freshly eroded channel segments, migrating sinuous curves, channel  
30 abandonment, and lobate deposits. We also observed early stages of gully initiation,  
31 demonstrating that these processes are not merely modifying pre-existing landforms. The  
32 timing of activity closely correlates with the presence of seasonal CO<sub>2</sub> frost, so the  
33 current changes must be part of ongoing gully formation that is driven largely by its  
34 presence. We suggest that the cumulative effect of many flows erodes alcoves and  
35 channels and builds lobate aprons, with no involvement of liquid water. Instead, flows  
36 may be fluidized by sublimation of entrained CO<sub>2</sub> ice or other mechanisms. The frequent  
37 activity has likely erased any features dating from high-obliquity periods, so fresh gully  
38 geomorphology at middle and high latitudes is not evidence for past liquid water. CO<sub>2</sub>  
39 ice-driven processes may have been important throughout Martian geologic history, and  
40 their deposits could exist in the rock record, perhaps resembling debris-flow sediments.

41

42 Gully landforms on Mars resemble water-formed features on Earth, with channels  
43 transporting material from an alcove to a depositional apron. From their discovery (Malin  
44 and Edgett, 2000), they have generally been interpreted as evidence for wet debris flows  
45 or flowing liquid water (e.g., Carr, 2006). Such liquid would have major implications for  
46 Martian climate, geology, the possibility of life, and the definition of Special Regions for  
47 planetary protection (Rummel et al., 2014). Understanding the formation of gullies has  
48 thus been a major focus of recent Mars science, as shown by the work in this volume.

49 Numerous hypotheses for gully formation have been considered. Martian surface  
50 conditions are not favorable for the existence of liquid water, so initial models focused on  
51 release of groundwater from shallow or deep aquifers (Malin and Edgett, 2000; Mellon  
52 and Phillips, 2001; Gaidos, 2001), possibly aided by geothermal heating melting  
53 permafrost (Hartmann, 2001; Hartmann et al., 2003) or the occurrence of brines (Knauth  
54 and Burt, 2002). However, the occurrence of gullies on sand dunes and isolated peaks  
55 argued against significant input from aquifers, and led to the development of models  
56 based on insolation-driven melting of snow or shallow permafrost at times when the  
57 obliquity of Mars was high (Lee et al., 2001; Costard et al., 2002; Gilmore and Phillips,  
58 2002; Hecht, 2002; Christensen, 2003; Hartmann et al., 2003; Williams et al., 2009).  
59 Alternative processes were considered, such as release of liquid CO<sub>2</sub> from the subsurface  
60 (Musselwhite et al., 2001), various CO<sub>2</sub> frost-based hypotheses (e.g., Hoffman, 2002;  
61 Ishii and Sasaki, 2004; Ishii et al., 2006), or purely dry flow with no volatile involved  
62 (Treiman, 2003; Shinbrot et al., 2004), but were generally considered unlikely due to the  
63 morphologic similarity between Martian gullies and water-formed terrestrial features.

64           New flows were discovered in gullies by the Mars Orbiter Camera (MOC) on the  
65 Mars Global Surveyor mission (Malin et al., 2006). Later observations showed that the  
66 activity is seasonal (Harrison et al., 2009; Dundas et al., 2010), and at several locations  
67 changes in gullies have been tightly constrained to occur around the time that seasonal  
68 frost is present, indicating that they are driven by the frost (Reiss et al., 2010; Diniega et  
69 al., 2010; Dundas et al., 2012; 2015b; Raack et al., 2015). Although seasonal melting of  
70 H<sub>2</sub>O frost was noted as a possible cause of activity (Reiss et al., 2010), CO<sub>2</sub> frost is much  
71 more abundant on Mars (e.g., Leighton and Murray, 1966). In combination with the  
72 occurrence of assorted defrosting features in some gullies, this led Diniega et al. (2010)  
73 and Dundas et al. (2010; 2012; 2015b) to suggest that CO<sub>2</sub>-driven processes were  
74 responsible for the current activity, a possibility foreshadowed by early reports of CO<sub>2</sub>  
75 defrosting and possible flow features in gullies (Bridges et al., 2001; Hoffman, 2002;  
76 Hansen et al., 2007; Mangold et al., 2008). In a captioned image release, Malin and  
77 Edgett (2005) also suggested that CO<sub>2</sub> frost could be involved in an early example of  
78 dune gully activity. Diniega et al. (2010) and Dundas et al. (2012; 2015b) argued that the  
79 current activity could be actively forming dune gullies and “classic” Martian gullies, and  
80 not merely modifying older water-formed features.

81           Seasonal frost deposits are prominent at middle and high latitudes on Mars. The  
82 CO<sub>2</sub> caps extend only to around  $\pm 50^\circ$  latitude (e.g., Piqueux et al., 2015), poleward of  
83 many gullies. However, localized frost on slopes occurs closer to the equator, at latitudes  
84 where gullies are common. Recent mid-latitude surveys include examinations of Mars  
85 Orbiter Camera (MOC) images by Schorghofer and Edgett (2006), and of near-IR  
86 spectral data by Vincendon et al. (2010a, 2010b). Schorghofer and Edgett (2006)

87 observed frost at latitudes as low as 24°S, which they interpreted as CO<sub>2</sub>, although  
88 visible-wavelength images cannot distinguish composition. Vincendon et al. (2010a,  
89 2010b) reported detections of CO<sub>2</sub> frost at latitudes as low as 34° S, and water frost  
90 reaching 13°S and 32°N. This hemispheric asymmetry in the occurrence of low-latitude  
91 frost, also observed by Schorghofer and Edgett (2006), is caused by the occurrence of  
92 southern winter solstice near aphelion, which makes the winter longer and colder. Dundas  
93 et al. (2015b) reported a similar asymmetry in gully activity. Vincendon (2015) examined  
94 near-infrared spectra of active gullies, and found that most were consistent with the  
95 presence of CO<sub>2</sub> frost at the time of gully activity. However, the relatively-bright gully  
96 deposits were reported to form at times and places where H<sub>2</sub>O ice was expected but CO<sub>2</sub>  
97 was less probable.

98         A variety of frost-driven hypotheses have been proposed to explain gully  
99 formation or activity. Hecht (2002) suggested that abrupt heating of water frost could  
100 enable it to melt before sublimating, providing a source of liquid. Kossacki and  
101 Markiewicz (2004) modeled this process and proposed that melting could occur at a  
102 given location on a single day of each Mars year, but only in trace amounts. CO<sub>2</sub>-driven  
103 hypotheses have also been considered. Hoffman (2002) argued that basal sublimation  
104 beneath CO<sub>2</sub> could trigger mass movements, by avalanching and/or gas-lubricated flows.  
105 Ishii and Sasaki (2004) and Ishii et al. (2006) also proposed that CO<sub>2</sub> frost could  
106 avalanche, eroding the surface and forming gullies. They suggested that this was  
107 consistent with the orientations and global distribution of recent gullies, which closely  
108 matched models for seasonal CO<sub>2</sub> condensation. Hugenholtz (2008) suggested frosted  
109 granular flow, whereby a small amount of surface frost reduces friction and enables

110 granular flows. Cedillo-Flores et al. (2011) argued that sublimating CO<sub>2</sub> could fluidize  
111 overlying material, although they did not address the initial burial of the ice. Diniega et  
112 al. (2013) suggested a model of sliding CO<sub>2</sub> blocks for “linear” gullies on sandy slopes.  
113 Pilorget and Forget (2016) modeled CO<sub>2</sub> ice on gully slopes, and suggested that the  
114 pressure rise from basal sublimation was capable of fracturing the ice and triggering mass  
115 movements.

116 We analyzed the distribution of seasonal frost in the mid-latitudes in high-  
117 resolution color images. This enables a meter-scale understanding of the behavior of the  
118 frost and its association with landforms. We compare these frost data with observations  
119 of gully activity and its morphological effects, expanding the survey of Dundas et al.  
120 (2015b). Finally, we discuss the implications of this work for the formation and evolution  
121 of gullies on Mars.

122 Following common practice, we use the term *gully* or *gully landform* for the  
123 alcove-channel-apron assemblages on Mars reported by Malin and Edgett (2000),  
124 although under terrestrial definitions (e.g., Neuendorf et al., 2005) “gulch” or “ravine”  
125 would be more accurate for many of these kilometer-scale features. Additionally,  
126 although terrestrial “debris flows” are commonly defined as wet flows with a wide range  
127 of grain sizes (e.g., Iverson, 1997; Turnbull et al., 2015), this usage is not always  
128 followed in planetary science, so we refer to “wet” or “aqueous” debris flows to  
129 emphasize this aspect. We use the Mars Year calendar defined by Clancy et al. (2000).  
130 Seasons are referred to by the areocentric longitude of the sun ( $L_S$ ), where  $L_S=0^\circ$  is the  
131 northern vernal equinox. Mars Year 0 (MY 0) began at  $L_S=0^\circ$  on May 24, 1953.

132

133 **Data and Methods**

134 *Data*

135         The primary data set for this work was images acquired by the High Resolution  
136 Imaging Science Experiment (HiRISE; McEwen et al., 2007) on board the Mars  
137 Reconnaissance Orbiter (MRO) spacecraft (Zurek and Smrekar, 2007). HiRISE images  
138 are typically 5–6 km wide, with a central swath in three colors (red, blue-green (BG), and  
139 near-infrared) in the central 20% of the image, and a pixel scale of 25–60 cm. Delamere  
140 et al. (2010) provide more information about HiRISE color imaging. The Reduced Data  
141 Records (RDRs) used in this study are map-projected at a scale of 25 or 50 cm/pixel (or  
142 rarely 1 m/pixel). The Sun-synchronous MRO orbit constrains the local time for mid-  
143 latitude images to be near 3 PM. Incidence angles vary primarily with season.

144

145 *Frost Survey*

146         In order to survey mid-latitude frost, we selected a data set from HiRISE images  
147 acquired before  $L_S=0^\circ$  of MY 33, roughly 4.5 MY after the start of the MRO mission.  
148 (Transition Orbit imaging occurred between  $L_S=114\text{--}116^\circ$  of MY 28, and Primary  
149 Science Phase began at  $L_S=132^\circ$ .) The images were chosen from the HiRISE “science  
150 themes” of Seasonal, Mass Wasting, Fluvial, and Impact Processes (McEwen et al.,  
151 2007). These themes were selected because they specifically target gullied locations and  
152 other steep slopes such as fresh craters with repeat coverage. Some gullies or steep slopes  
153 occur in other themes, but these constitute a sufficient sample. Images with significant  
154 atmospheric haze were discarded. We chose data from an envelope of latitude and  $L_S$  that  
155 encompasses the infrared observations of water frost by Vincendon et al. (2010a) for

156 latitudes 25° - 60° in each hemisphere. This encompasses the range of most “classic”  
157 gullies, including those with well-studied activity. Water frost is also observed at lower  
158 southern latitudes (Vincendon et al., 2010a), and some equatorial gullies have been  
159 documented (e.g., McEwen et al., 2014; Auld and Dixon, 2016), but their activity has not  
160 been well studied. We focused on the mid-latitudes for the present study, and discuss the  
161 implications for equatorial gullies below. Frost is especially abundant in polar gullies.

162         We used only the color RDR observations, because frost can be indistinct in the  
163 red filter-only portion of the image (i.e., although it is often possible to determine that  
164 frost is present in the red-filter images, it is difficult to be confident that it is not present  
165 when not observed). With only three color bands, it is difficult to conduct an automated  
166 search for spectral features of H<sub>2</sub>O or CO<sub>2</sub> frost in HiRISE data. Color ratios and  
167 brightnesses characteristic of frost in the BG bandpass may not be sufficiently unique for  
168 confident identification, especially in shadows or for small frost patches, which are some  
169 of the cases of most interest here. (An automated frost-detection algorithm developed by  
170 the HiRISE team for use in color adjustments is generally successful but commonly  
171 misses small frost patches or those in shadow.) The large size of the images also makes it  
172 impractical to manually search the entirety of every image at full resolution, even in our  
173 limited data set. Instead, we focused on the upper parts of steep slopes, particularly those  
174 with gullies as well as non-gullied slopes of a similar size and (apparent) steepness.  
175 Images lacking such slopes were ignored. We also excluded sites with excessively  
176 complex topography (such as certain rugged crater central peaks), because those sites are  
177 time-consuming to search, have ambiguous slope orientations when stereo data are not  
178 available, and may have unusual thermal environments due to complex slope interactions.



179 These considerations also led to the exclusion of dune field slopes. Impact craters less  
180 than 1 km in diameter were also omitted; frost and gullies do occur in such craters and on  
181 dunes, but this provided an objective cutoff and limited the data set to a manageable size.  
182 The resulting data set is dominated by impact crater slopes, with a few other significant  
183 scarps included.

184         Once these constraints were applied, we examined the remaining steep slope  
185 segments at the full RDR resolution to look for frost. Images were locally stretched as  
186 needed to enhance the color contrast, including in shadows. Although many cases are  
187 obvious, small patches of trace frost require some interpretation to rule out the presence  
188 of relatively-bright, relatively-blue lithic material. We interpreted as frost any surface  
189 material that appears distinctly “white” or bright “blue” in a stretched three-color HiRISE  
190 image (i.e., bright in all three bands or in the blue-green band), and that does not appear  
191 to be rock, sand, etc., based on morphology and geologic setting. (For instance,  
192 relatively-blue material dominating an equator-facing slope is unlikely to be frost except  
193 in cases where frost is ubiquitous. Sand deposits are likely to be rippled and relatively  
194 dark.) Frost commonly has very strong associations with small-scale topography, so  
195 bright material fringing topographic features or occupying particular slope facets is likely  
196 to be frost. For some uncertain cases where summer images were available, we compared  
197 the two. Features that persisted in summer images were assumed to be relatively-blue  
198 lithic material, although it is possible that in rare instances perennial ground ice could be  
199 exposed. Distinguishing diffuse frost from atmospheric haze can also be problematic, but  
200 the latter is indifferent to surface topography. In some cases, we interpret other coloration  
201 as frost based on context. The most common of these was in times and places where frost

202 is very widespread, and may be translucent and/or dirty in the area of interest. In  
203 combination with a lack of defrosted surfaces for contrast, this can make frost coloration  
204 less distinctive. With only three broad color channels, it was not possible to distinguish  
205 between H<sub>2</sub>O and CO<sub>2</sub> frost.

206         Slopes were divided into eight 45° octants and we recorded the presence or  
207 absence of frost on slopes in each octant in each image. We subdivided these  
208 observations into alcove and non-alcove slopes, where alcove slopes are the interiors of  
209 moderately- to well-developed gully or gully-like alcoves. Shallow alcoves and other  
210 slope irregularities were grouped with non-alcove slopes. Since high-resolution  
211 topography is only available for a small fraction of sites, slope direction was estimated  
212 from the RDR images. In cases where a slope was predominantly facing direction X but  
213 just barely curved into the next octant, only direction X was recorded. This ensured that  
214 those small slivers, which do not fully capture the frost conditions for their nominal slope  
215 orientation, would not be an excessive fraction of the data. The relevant direction is the  
216 downhill orientation of the slope on the scale at which gullies develop, because we are  
217 interested in the geomorphic evolution of gullies. For instance, a hollow with frost on a  
218 small southward slope facet of a generally east-facing slope was recorded as east-facing  
219 frost, because such frost could contribute to the formation of east-facing gullies. We also  
220 noted the presence of spots or flows superposing the frost, associated with active  
221 defrosting (cf. Kieffer, 2007; Hansen et al., 2010; Thomas et al., 2010).

222         Some of the seasonal ice that we classified as frost may actually have been  
223 deposited by precipitation, as snow. Snowfall contributes an estimated 3–20% of the  
224 mass of the CO<sub>2</sub> cap at 70–90°S latitude (Hayne et al., 2014). We have no reliable way to

225 distinguish the two in HiRISE data, and refer to all seasonal ice as frost in order to  
226 distinguish it from ground ice, which is also likely present in the subsurface near many  
227 gullies.

228         Some frost was likely missed by this survey, for several reasons. Small frost  
229 patches or diffuse thin frosts might not produce distinct color and albedo changes, and  
230 dust could also reduce the contrast. Frost can also be transparent or translucent at visible  
231 wavelengths under some conditions. Additionally, frost in shadow can be more difficult  
232 to recognize due to illumination by scattered light only. We recorded frost as possible in  
233 cases where there were candidate patches but we were not confident of the interpretation.  
234 This most commonly occurred in shadows or small diffuse patches. If the image quality  
235 in shadow was too poor for any useful interpretation, the shadowed slope was excluded.

236

### 237 *Gully Activity Survey*

238         We updated the gully activity survey of Dundas et al. (2015b) with 1.5 Mars years  
239 of additional data, through MRO orbit 48999. This both added many new monitoring  
240 sites and extended the time record for many individual gullies. In a handful of cases, we  
241 have not used the most recent available image, generally because it was poorly  
242 illuminated. The methods follow those in Dundas et al. (2015b). Briefly, HiRISE images  
243 of the aprons and lower channels at a reduced resolution of 1 m/pixel were blink-  
244 compared to look for changes. Monitoring sites are those gully sites poleward of 25°  
245 latitude in each hemisphere with HiRISE image coverage separated by at least 4000  
246 MRO orbits (roughly ten months). Images from each site were compared against the most  
247 similar older images to produce optimal comparisons spanning the full time interval for

248 each site. Although in some instances the lighting and image geometry were significantly  
249 different, it is possible to detect changes even in non-ideal cases. However, some number  
250 of changes are missed. This is emphasized by the occasional observation of changes that  
251 can be dated with older images, but only after they are detected in more recent data with  
252 better conditions for comparison. This is an inherent limitation of the data and implies  
253 that the activity rates here are a lower bound. Thin, transient albedo changes with no  
254 meter-scale topographic effects are particularly likely to be missed, but more substantial  
255 changes may be unseen (or not considered confirmed) when the available images have  
256 dissimilar lighting or viewing geometry.

257         Martian gullies (Fig. 1) are often divided into dune gullies and non-dune gully  
258 landforms. Dune gullies have often been neglected in efforts to understand the formation  
259 of “classic” gullies (alcove-channel-apron morphology) on crater walls and other steep  
260 slopes. “Linear dune gullies” like those in Russell crater (Mangold et al., 2003; Reiss and  
261 Jaumann, 2003) do have a distinctive appearance in that they lack aprons and often have  
262 terminal pits (Fig. 1e), but many dune gullies have the classic alcove-channel-apron  
263 morphology (Fig. 1f). Additionally, dune and non-dune gullies are more gradational than  
264 commonly appreciated (Fig. 1b-d). Here we have included the gradational forms with the  
265 main survey. Both types of dune gully are commonly active, and due to the number of  
266 changes we did not attempt to catalog all events on the dunes. However, dune gullies  
267 with classic morphology likely form by the same processes as similar crater-wall gullies,  
268 so we document several examples with prominent morphologic changes.

269

270 **Observations**

271 *Frost Survey*

272           The southern-hemisphere seasonal frost distribution in HiRISE data (Fig. 2) is  
273 broadly consistent with the observations of water frost by Vincendon et al. (2010a).  
274 Those water frost observations approximately define the occurrence envelope of seasonal  
275 frost on Mars, because water ice has a broader spatial and temporal distribution  
276 (Schorghofer and Edgett, 2006; Vincendon et al., 2010a, b). However, CO<sub>2</sub> dominates the  
277 mass percentage of the frost except at the very fringes of CO<sub>2</sub> deposition (e.g., Leighton  
278 and Murray, 1966; Vincendon, 2015), as the minor atmospheric species H<sub>2</sub>O forms only  
279 very thin deposits at any latitude. Some seasonal water frost occurs at lower latitudes than  
280 the 25°S cutoff in this study (Vincendon et al., 2010a). The relationship between frost  
281 and slope orientation is as expected: frost was most commonly observed on pole-facing  
282 slopes, and the spatial and temporal occurrence expands at higher latitudes. Frost is  
283 strongly affected by topography even at very small scales, occurring in the most-sheltered  
284 slope facets. Such local effects enable frost to occur even on broadly equator-facing  
285 slopes (Fig. 3).

286           We did not include the highest-latitude gullies in this survey because images are  
287 concentrated at only a few locations. However, those locations have been imaged  
288 frequently and demonstrate widespread defrosting spots and flows (Fig. 4; see also  
289 Dundas et al., 2012). Sublimation activity at particular locations is similar from year to  
290 year, but does not repeat exactly.

291           Defrosting spots and flows occur in the latter part of the frost season, as the frost  
292 is being removed. These sublimation features were most commonly observed at higher

293 latitudes, and are rare equatorward of  $\sim 40^\circ\text{S}$ . Defrosting spots and flows commonly show  
294 a strong concentration within alcoves and channels.

295 Data in the northern hemisphere were sparse due to the lower abundance of  
296 gullies and steep slopes on the northern plains. Frost was only observed poleward of  
297  $\sim 35^\circ\text{N}$ , consistent with near-infrared spectral observations of water frost by Vincendon et  
298 al. (2010a). Defrosting spots and flows are also rare.

299

### 300 *Gully Change Survey*

301 The extended change survey (Fig. 5) reveals that gully activity is common,  
302 particularly in gullies in the southern highlands. Over the full monitoring survey, 20% of  
303 gully sites south of  $25^\circ\text{S}$  have shown activity with before-and-after HiRISE coverage,  
304 compared with 5% north of  $25^\circ\text{N}$ , and multiple events at particular sites are more  
305 common in the south as well. The number of winter solstices spanned by HiRISE  
306 observations was 2.9 per site in the southern hemisphere, compared with 2.5 in the north,  
307 so northern activity may be slightly underrepresented but not by enough to explain this  
308 difference. These figures include gullies on sand-covered non-dune slopes, but not dune  
309 gullies. Monitoring sites are preferentially those with fresh gullies and steep slopes,  
310 which are likely to be the most active, but do include less pristine gullies as well.  
311 (Possible biases are discussed extensively in Dundas et al. (2015b); the expanded data set  
312 herein has the same general characteristics.) In addition to being more frequent, activity  
313 in the south is more geomorphically effective, as most of the observed changes in the  
314 north are superficial (little or no topographic change resolvable by HiRISE). Several sites  
315 and even individual gullies have experienced multiple flows (at least sixteen mass

316 movements have occurred in Gasa crater over five Mars years), but the overall level of  
317 activity suggests that recurrence intervals in individual gullies are on the order of  
318 centuries. Dune gullies are particularly active, with annual changes in some cases, but  
319 numerous non-dune gully sites have also seen repeated changes. The timing of some  
320 flows can be constrained to within a few weeks, while other intervals span a Mars year or  
321 more. When well-constrained, gully activity is closely correlated with seasonal frost,  
322 particularly the latter part of the frosted season (Fig. 6).

323         The features of the various gully changes are diverse. The mass movements range  
324 from barely resolved to kilometers long, from superficial albedo changes to major erosion  
325 and deposition, and can be bright, dark, colorful, or neutral in tone. Here we describe  
326 flows from source to sink and the various morphological effects that occur, with the  
327 understanding that there are exceptions to most general statements. Additional examples  
328 of changes are shown in the following section.

329         The detectable sources of individual events are usually small and indistinct. We  
330 search for changes by making comparisons of the aprons and channels, where they are  
331 most visible. When events were traced up towards the source, the effects typically  
332 become more subtle, and may appear disconnected, although it is likely that there are  
333 simply unresolved changes uniting the flow, or the flow passed through with little effect.  
334 The typical plan form is best seen by examining flows that have covered or disturbed  
335 seasonal frost, which makes the entire shape of the flow distinct even where erosion and  
336 deposition are superficial (Fig. 7). These flows were virtually point-source features,  
337 which descended down channels before producing much larger terminal effects. Some

338 flows do have larger, distributed source areas, although this could represent collapse  
339 propagating from a smaller initial failure.

340 Lower in the flow path, the morphological effects become more prominent.  
341 Changes in the channels are common. Some of these are obviously erosive or  
342 depositional, although in other cases there are distributed changes that have clearly  
343 altered the morphology but where the net local effect is not clear at HiRISE resolution.  
344 However, the formation of terminal deposits requires that material be eroded further up  
345 the slope, so the overall effect is to erode material from the alcoves and/or channels,  
346 resulting in net transport down the channel bed to the apron. Transport and deposition of  
347 meter-scale boulders is common in the larger events.

348 Deposition occurs in the lower reaches of the flows. Sometimes deposits end  
349 within existing channels; others reach beyond and onto the apron. The deposits are highly  
350 variable: some form thick lobate deposits, while others appear superficial at HiRISE  
351 resolution. The flows can deposit boulders or bury existing rocks in finer material, so  
352 boulder density is not necessarily an indicator of freshness or rock breakdown (as  
353 proposed by de Haas et al., 2013). Lobate features are not necessarily at the farthest point  
354 of the deposit, and disturbances and changes can reach beyond obvious lobate flows. The  
355 deposits can be brighter or darker than their surroundings, but can also be near-neutral in  
356 HiRISE red-filter images. Likewise, some deposits are distinct in color while others  
357 closely match the existing surface. Deposits that appear relatively-blue in HiRISE  
358 enhanced color are almost always darker than their surroundings in the red-filter images,  
359 while those that appear yellow are brighter.



360 Flows retain distinct color or albedo for varying lengths of time. For instance, the  
361 two bright deposits reported by Malin et al. (2006) formed no later than MY 27 and  
362 remained obvious in HiRISE images from MY 33. Other flows mostly fade within a Mars  
363 year, reflecting more effective local resurfacing, likely dust deposition. Some flows are  
364 only distinct while shadowed (Dundas et al., 2012; 2015b). These are demonstrably  
365 active events because the patterns change from year to year at individual sites, despite  
366 similar lighting. However, they have unresolvable effects on the color and relief of the  
367 surface. Other, similar flows are most distinct in winter shadow but produce very minor  
368 changes in well-lit images, demonstrating a gradation with more typical activity. Such  
369 flows may be minor activity that was distinct because of contrast with traces of frost,  
370 analogous to the more obvious flows over frost observed elsewhere (Fig. 7), but produce  
371 changes that are minimal at HiRISE resolution in well-illuminated images. Alternatively,  
372 they could be extremely thin flows that produced only short-term albedo differences.  
373 They may be under-reported because we have not searched for them in all shadowed  
374 images, as well as the inherent difficulty of observing features in deep shadow.

375 Although most of the changes occurred within defined gullies, some appear to be  
376 the initial stages of gully formation. A pair of flows in Raga crater followed a crease in  
377 the topography, which was so ill-defined in the earliest images of the site that it would  
378 likely have been omitted by gully surveys. After two events, the channel became notably  
379 more visible and connected (Fig. 8), progressing towards the appearance of better-defined  
380 gullies a short distance away. Both of these changes occurred in fall or winter, making  
381 them quite distinct from the Recurring Slope Lineae (RSL) found in the same crater in  
382 the warm seasons on more equator-facing slopes (McEwen et al., 2011).

383 Dune gullies appear to be the most active and experience the largest changes  
384 (Diniaga et al., 2010). For example, a single large dune gully in Matara crater (Fig. 1f)  
385 has experienced major mass movements in every winter since the start of HiRISE  
386 observation. Such gullies can be fundamentally reworked within a few years. Fig. 9  
387 shows a gully on a large dune west of the Argyre basin. Over three Mars years, the  
388 system transitioned from a degraded alcove and infilled channel to a sharp, fresh alcove  
389 feeding a 500-m-long, 20-m-wide, terraced channel.

390

### 391 **Interpretation**

#### 392 *Processes Causing Current Activity*

393 The timing of numerous well-constrained gully events points to seasonal frost as  
394 the cause or trigger for current flows in gullies. Other possible seasonally-controlled  
395 drivers are inconsistent with the observed temporal behavior. Groundwater release could  
396 be seasonal, but should favor summer (Goldspiel and Squyres, 2011) and is extremely  
397 unlikely on sand dunes or isolated peaks. Aeolian processes are most active at maximum  
398 atmospheric pressure, during southern summer (Ayoub et al., 2014). RSL are most active  
399 in the warmest seasons (McEwen et al., 2011; 2014). These options are out of phase with  
400 the season of most observed gully flows. In contrast, the observed timing of activity is  
401 highly correlated with the presence of seasonal frost.

402 Fine details of the distribution of visible frost further support seasonal frost as the  
403 trigger for activity. Penticton crater has frost on a broadly equator-facing slope at an  
404 unusually low latitude (38.4°S), and a rare example of an equator-facing new gully  
405 deposit at that latitude (Fig. 3). This coincidence suggests that the frost could have been

406 the trigger for the Penticton flow. The steep slopes and morphology of the deposit are  
407 considered consistent with dry flow (Pelletier et al., 2008), so a trigger by this small  
408 amount of frost is possible. If this is the case, the minimum frost amount required to  
409 trigger mass movements may be very low, but with only one example we cannot establish  
410 whether this flow was caused by frost or was simply a random volatile-free event.  
411 Volatile-free mass wasting must occur on Mars and a few likely examples have been  
412 observed outside of gullies, but the frequency is unknown.

413         Liquid flow due to melting water frost is excluded as the cause of current  
414 changes, for several reasons. First, melting is extremely difficult on present-day Mars.  
415 Ingersoll (1970) pointed out that the latent heat losses to sublimation are so high that  
416 insolation at the orbit of Mars is insufficient to melt ice. Even at temperatures below 273  
417 K, the evaporative cooling removes more heat than can possibly be supplied by the Sun,  
418 precluding warming to the melting point. Hecht (2002) suggested that under certain  
419 circumstances (rapid heating, a lowered melting point, and low effective emissivity due  
420 to heat input from alcove walls), water ice could be melted. Kossacki and Markiewicz  
421 (2004) modeled such a scenario and suggested brief melting episodes during defrosting,  
422 producing  $<1 \text{ kg/m}^2$  of melt. However, their model significantly underestimates  
423 evaporative cooling since it included only forced-convection (wind-driven) sublimation.  
424 For the assumed wind speed of 5 m/s, free convection is a factor of 2–4 stronger at 270  
425 K, depending on the atmospheric pressure (cf. Dundas and Byrne, 2010). This is likely to  
426 prevent even this limited melting. Second, the atmospheric pressure at many of the active  
427 locations is below the triple point pressure. Finally, the expected thickness of H<sub>2</sub>O frost  
428 deposits is small, likely no more than a fraction of a millimeter (Vincendon et al., 2010b;

429 Vincendon, 2015). Such negligible amounts would not flow through or over a porous  
430 medium even if they melt somehow.

431         Boiling of small volumes of brine in the shallow subsurface (Massé et al., 2016) is  
432 possible, if the brine is present and does not evaporate. (Melting and boiling pure  
433 subsurface ice suffers from the same difficulties as surface frost.) Conditions for  
434 deliquescence to produce such brine occur on Mars (e.g., Gough et al., 2011), but if such  
435 brines form from deliquescence, the available volumes would be extremely limited  
436 because the Martian atmosphere is very dry, and in the winter H<sub>2</sub>O will be cold-trapped at  
437 the surface rather than in the subsurface. If such a process occurs on Mars, it is likely to  
438 involve much less water than the flows generated in the laboratory by Massé et al.  
439 (2016), but could serve as a trigger for dry flows. However, it should not occur when CO<sub>2</sub>  
440 ice is present on the surface, which buffers the local temperature to the frost point; CO<sub>2</sub>  
441 was definitely present for some of the observed activity with the best time constraints. In  
442 sum, the strength of the deliquesced brine for realistic Martian conditions is unknown,  
443 and the seasonal timing of activity does not support this process in gullies. Instead, it is  
444 likely that activity is caused by processes with no melting or liquid present.

445         Pilorget and Forget (2016) modeled the possibility that basal sublimation and  
446 rising pressure beneath CO<sub>2</sub> ice trigger gully activity, developing an idea considered by  
447 Hoffman (2002) and Ishii et al. (2006); this is essentially the “Kieffer model” that  
448 produces high-latitude defrosting spots (e.g., Kieffer, 2000; 2007; Piqueux et al., 2003;  
449 Hansen et al., 2010; Thomas et al., 2010). However, gully activity is common between  
450 30–40°S, where we rarely observed defrosting spots or flows. Does this contradict the  
451 basal sublimation model? It is possible that at lower latitudes, spots are small or short-

452 lived and difficult to observe, particularly in the shadowed, rugged topography of gullies.  
453 It is also possible that gas ejection in gullies rarely moves silicate material—steep alcoves  
454 may have smaller amounts of loose fine material than the polar regions. In this case, gas  
455 ejection might have no tangible effect except when it triggers rare, stochastic, larger-scale  
456 failures leading to the observed mass movements. The model is supported in higher-  
457 latitude gullies, where spots and flows are common and recur every Mars year (Fig. 4;  
458 see also Dundas et al. (2012)). These flows can be considered bedload transport along a  
459 channel, albeit in unfamiliar form. The volumes transported annually may be small (the  
460 flows have no visible relief in HiRISE images), but the high frequency could make this a  
461 significant process in gully evolution where it occurs.

462         Although the basal sublimation model is consistent with activity in high-latitude  
463 gullies and can potentially cause lower-latitude activity, it is probably not the only  
464 significant frost process. The small abundances and patchy distribution of the lower-  
465 latitude frost are not conducive to gas trapping, and may prevent the CO<sub>2</sub> pressurization  
466 process from being as efficient as modeled. Additionally, Vincendon (2015) reported that  
467 some gullies with activity, particularly those with bright deposits, have H<sub>2</sub>O frost but no  
468 detectable CO<sub>2</sub>. CO<sub>2</sub> may yet be detected by future observations of those sites, occur at  
469 night (cf. Piqueux et al., 2016) or in unresolved patches, or be concealed by coatings of  
470 water frost. However, the occurrence of gully activity at locations where frost abundances  
471 are low suggests that other trigger mechanisms contribute to activity; these are not  
472 mutually exclusive. The point-source initiation of some flows that disturb frost (Fig. 7)  
473 suggests avalanching (cf. Hoffman, 2002; Ishii and Sasaki, 2004; Ishii et al., 2006). This  
474 could occur within granular frost without any gas pressure, although gas pressure would

475 be an effective way to trigger avalanches (Hoffman, 2002; Ishii et al., 2006). Another  
476 possibility is frosted granular flow (Hugenholtz, 2008), although the morphology of  
477 terrestrial examples is a poor match for Martian gullies (Harrison, 2016). Slope failures  
478 might also be triggered by deposition and sublimation of small amounts of frost on steep  
479 alcove slopes, picking up material as they descend. Such a process would be more  
480 effective if any frost is deposited between the grains, so that sublimation can dislodge  
481 material (cf. Sylvest et al., 2016), and might be most effective in early or late winter  
482 when frost is patchy and has uneven effects on the surface.

483         Why do CO<sub>2</sub>-triggered gully flows produce morphologies distinct from typical  
484 terrestrial mass wasting? One possibility is that terrestrial geomorphologies are  
485 dominated or overprinted by other processes. Another possibility is that gas fluidization  
486 from frost makes the flows more mobile than simple granular flow, as suggested by  
487 Hoffman (2002). Cedillo-Flores et al. (2011) showed that sand or dust superposed on top  
488 of CO<sub>2</sub> frost on Mars could be fluidized by sublimation driven by heat fluxes of tens of  
489 W/m<sup>2</sup>, at which point the upward gas flow overcomes the weight of the particles.  
490 However, their model proposed that the mobilized material was aeolian sediment  
491 superposed on the frost and heated by the Sun. This resembles the behavior of defrosting  
492 flows creeping within some gullies (Fig. 4), but is unlike the observed point-source flows  
493 modifying bare frost (Fig. 7) and has no mechanism for erosion of the surface. To date,  
494 we have not observed any indication that aeolian processes are an important precursor to  
495 gully mass movements in general (as proposed by Treiman (2003)), although sand  
496 movement certainly affects dune gullies. Some flows clearly mobilize boulders, not just  
497 aeolian materials. Pilonget and Forget (2016) suggested that the gas generated by basal

498 sublimation underneath frost could also serve to fluidize the flows, but there are few  
499 defrosting spots in the lower-latitude active gullies. Additionally, some activity occurs in  
500 early winter while CO<sub>2</sub> is condensing and gas pressure should be low.

501         We suggest a related alternative, in which gas generation occurs via two effects  
502 within a mix of sediment and CO<sub>2</sub> ice tumbling down a gully. First, the potential energy  
503 of falling material is initially converted to kinetic energy but must ultimately dissipate as  
504 heat (Iverson, 1997), or latent heat loss (sublimation) if buffered at the CO<sub>2</sub> frost point  
505 temperature. The available energy is 3.7 J/kg per meter of descent, for Martian gravity.  
506 For a typical vertical fall of 300 m, this amounts to 1100 J/kg. Second, eroded sediment  
507 from the shallow subsurface will be at least slightly warmer than the ice (especially if gas  
508 pressure has risen, causing a higher frost point), and could cause additional sublimation  
509 (Hoffman, 2002). Warmer material can also be entrained when flows pass into unfrosted  
510 areas. Mixing within the falling material will allow this heat to be transferred to the CO<sub>2</sub>  
511 frost, causing sublimation. Lithic material at only a few K above the frost point  
512 temperature could make several thousand J/kg available, and defrosted areas could be  
513 tens of degrees warmer. Hence, this is potentially even more important than the kinetic  
514 energy effect, and dramatically so in conditions where the flow is able to incorporate  
515 much warmer materials, although not all of the heat transfer need occur while the  
516 material is flowing. Thus, there is likely at least  $\sim 10^3$  J/kg of energy to be dissipated in  
517 typical gully flows, or  $\sim 10^6$  J/m<sup>3</sup> for a porous mixture of frost and lithic material. If the  
518 flow distance is 1 km at a velocity of 10 m/s (plausible values for gullies in Hale crater  
519 (Kolb et al., 2010a), which are now known to be active) then the heat used in gas  
520 generation could be up to 10<sup>4</sup> W/m<sup>3</sup>, producing a vapor flux equivalent to 10<sup>4</sup> W/m<sup>2</sup> for a

521 1-m-thick flow if all spent on sublimation. This is a highly transient phenomenon, so this  
522 power is only generated briefly. The high energy dissipation in the gully flows is possible  
523 because it is distributed through the entire volume of the flow, and is not a radiant heat  
524 flux, but it is converted to per-area units here for comparison with the values from  
525 Cedillo-Flores et al. (2011). Since we are estimating the energy directed into sublimation,  
526 equal energy fluxes imply identical gas fluxes. If no CO<sub>2</sub> were present and this energy  
527 was expended on warming lithic material rather than sublimating frost, the temperature  
528 rise during the flow would be <2 K. Sublimation could occur within the flow, or at the  
529 base if it runs over frost. There is undoubtedly some efficiency factor since not all energy  
530 will be expended on sublimation: some energy will be lost to the surroundings, and some  
531 kinetic energy could warm the lithic component of the gully flow out of equilibrium with  
532 the CO<sub>2</sub> ice. (However, acting in the other direction, addition of energy from warmer  
533 rocks and sediment could increase the gas generation by an order of magnitude or more  
534 over these estimates.) Moreover, the values suggested by Cedillo-Flores et al. (2011) are  
535 lower bounds on the flux needed in this scenario, since some of the gas is generated  
536 within the flow, which would cause a range in fluidity with height. However, if even a  
537 few percent of this energy goes into frost sublimation, the fluxes indicated by Cedillo-  
538 Flores et al. (2011) are easily exceeded, so some amount of fluidization is likely.  
539 Complete fluidization is not necessary to explain the Martian gully flows. The fan  
540 deposits of gullies are moderately steep and sometimes consistent with no gas fluidization  
541 (Kolb et al., 2010b), and it is likely that a spectrum of behaviors occurs even within  
542 individual gullies.



543           These processes represent a potential source of fluidization unknown in normal  
544 terrestrial mass movements, although they resemble processes that occur in ignimbrites  
545 and pyroclastic flows (cf. Branney and Kokelaar, 2002). We predict that, all else being  
546 equal, greater fluidization will correlate with thicker flows (greater gas flux per unit area,  
547 and gas escape timescales will follow the square of flow thickness per Darcy's Law),  
548 finer grain size (more effective transfer of heat from sediment to frost, greater ease of  
549 mobilization, and slower gas escape due to reduced permeability), flows that incorporate  
550 warm sediment well above the frost point (more likely later in the season), and flows with  
551 a greater vertical fall distance (more available energy per unit mass). Cohesion of dust  
552 and rapid cooling of small grains may reduce the effect of very fine grains (Cedillo-  
553 Flores et al., 2011). There may also be a correlation with a higher proportion of frost  
554 within the falling material, although if heat extraction from eroded material is important  
555 there might be an optimal ratio rather than a monotonic increase. High frost fractions  
556 could result in rapid (almost explosive) sublimation and high mobility similar to a  
557 suspension current, but might also result in swift gas loss causing the flow to stop. The  
558 frost/lithic ratio is not measurable with current data, but could correlate with latitude and  
559 season. Notably, of five gully sites studied by Kolb et al. (2010b), the highest-latitude site  
560 (at 46°S) had some of the most fluidized deposits. The efficiency factor is unknown and  
561 probably variable, depending on factors such as the grain sizes (also an important factor  
562 in the flux needed to cause fluidization) and the ratio of frost to lithic material.  
563 Experimental work is needed to determine how effective these processes would be under  
564 Martian conditions. Active fluidization during flow would have been difficult to observe  
565 in previous experiments on CO<sub>2</sub> frost flows (e.g., Sylvest et al., 2016), but those small-

566 scale experiments demonstrate that sublimation of CO<sub>2</sub> within sand can trigger flows on  
567 slopes well below the dynamic angle of repose.

568         In light of these observations, we propose the following model for the relationship  
569 between frost and gully activity. Gully mass movements are initiated by seasonal frost  
570 through several mechanisms. Of these, the defrosting-pressurization model suggested by  
571 Hoffman (2002) and Pilorget and Forget (2016) is directly supported in higher-latitude  
572 gullies, but other mechanisms are probably also involved at lower latitudes. Point-source  
573 flows resemble the initiation of avalanches, and small amounts of frost may be enough to  
574 trigger some activity simply by dislodging grains. Frost blocks and dark halos observed  
575 in linear gullies (Pasquon et al., 2016) (Fig. 10) suggest that that distinctive morphology  
576 is produced by sliding slabs of ice (Diniega et al., 2013). In other gullies, the relative  
577 importance of the various processes is probably variable, particularly as a function of  
578 latitude and other local conditions that affect frost condensation, such as alcove  
579 topography. These processes result in flows with varying mixtures of frost and entrained  
580 regolith descending down a channel, eroding and depositing in accordance with the flow  
581 velocity and interactions with local topography and overall slope. If small amounts of  
582 frost are capable of triggering mass movements, H<sub>2</sub>O frost may initiate flows in some  
583 cases, although not by melting. However, it would not be able to fluidize flows in the  
584 manner proposed for CO<sub>2</sub>, so such flows would behave like volatile-free mass  
585 movements. The correlation between CO<sub>2</sub> frost and prominent gullies suggests that CO<sub>2</sub>  
586 is much more important. This is unsurprising, since CO<sub>2</sub> frost is typically several orders  
587 of magnitude more abundant than H<sub>2</sub>O. Equatorial water frost does occur, as do  
588 equatorial gullies, but the latter are typically poorly developed and were not reported in a

589 global survey of 6 m/pixel Context Camera images (Harrison et al., 2015). The  
590 concentration of prominent gullies on mid-latitude pole-facing slopes is consistent with  
591 CO<sub>2</sub> as the major driver of erosion and cause of fluidized gully flows.

592 One northern-hemisphere gully alcove (Fig. 11) showed a pattern of spots with  
593 brightness and color suggestive of frost or ice, sufficiently late in the spring that frost is  
594 unlikely. The pattern of spots varies somewhat from year to year and the spots become  
595 less distinct over the spring. The alcove is cut into mid-latitude mantle material  
596 interpreted to be ice-rich (Conway and Balme, 2014), so it is likely that these exposures  
597 are subsurface H<sub>2</sub>O ice that is subsequently covered by a sublimation lag. This suggests  
598 that sublimation is an important secondary process in modifying some gully alcoves and  
599 liberating material for transport, as suggested by Forget et al. (2016). In such a process, a  
600 feedback between sublimation and CO<sub>2</sub>-driven transport could occur: frost-driven flows  
601 strip dry lag material above the ground ice, which subsequently sublimates until another  
602 lag develops. Gully locations cut into such ice-rich mantle deposits would thus be a form  
603 of sublimation-thermokarst, related to scalloped depressions (cf. Dundas et al., 2015a).

604

#### 605 *Morphological Effects of Current Activity*

606 Numerous morphologies observed in Martian gullies have been proposed to  
607 indicate that they are ultimately liquid water-formed features, regardless of the causes of  
608 current activity. These include sinuous, incised channels (Malin and Edgett, 2000;  
609 Mangold et al., 2010), braided or anastomosing channels (Malin and Edgett, 2000;  
610 Gallagher et al., 2011), terraces and longitudinal bars (Schon and Head, 2009), leveed  
611 lobate flows (Levy et al., 2010; Lanza et al., 2010; Johnsson et al., 2014; de Haas et al.,

612 2015b), longitudinal profile characteristics (Conway et al., 2015), and statistical  
613 parameterization of three-dimensional topography (Conway and Balme, 2016). However,  
614 the purported diagnostic nature of all of these features depends on experience with  
615 terrestrial analogs. *A priori*, we do not know what morphologies should be produced by  
616 flows triggered or enhanced by CO<sub>2</sub> frost, especially at Mars' gravitational acceleration,  
617 because the details of the processes are incompletely understood and we have no clear  
618 terrestrial analogs. Therefore, it is essential to understand what morphologies can be  
619 produced within currently-active features, which must be produced by frost-driven  
620 processes. Dundas et al. (2015b) showed new examples of several of these morphologies.  
621 Here we describe additional examples of newly formed morphologies in order to show  
622 that they can be created via current Martian surface processes.

623 Channel incision commonly occurs, particularly in the form of local erosion and  
624 channel extension or widening. It is extremely frequent and large-scale in dune gullies. In  
625 non-dune gullies, some clear examples were seen, such as erosion of a 50-m-long  
626 breakout from a preexisting channel (Dundas et al., 2015b); more commonly, the erosion  
627 is more subtle. Fig. 12a-b shows an example of extension of a pre-existing channel.  
628 Flows passing down the channel occasionally destabilize the slope, causing wall collapse  
629 and liberating material for future transport (Fig. 12c-d). Channel sinuosity also develops  
630 over time. In several cases, sinuous curves were observed to migrate and become more  
631 sinuous. The process involves erosion of the down-slope outside bank, suggesting that  
632 energetic flows strike the outside of the curve and enhance the curves in the channel as  
633 they are deflected. This does not continue indefinitely—we have also observed cutoff of a

634 sinuous curve (Fig. 13), analogous to the formation of an oxbow lake in a meandering  
635 stream.

636         Figure 14 shows an excellent example of current activity capable of producing  
637 complex, braided patterns. This location has a system of branching channels (Fig. 14a).  
638 These channels had faint bright material in an early HiRISE image (Fig. 14b), but in a  
639 later image have distinct bright deposits (Fig. 14c). A visible topographic change  
640 demonstrates that this is not simply a photometric effect. Instead, the older bright  
641 material represents a previous event following a similar pattern. The flows very likely  
642 had one source and branched downslope, although the source was not apparent. Within  
643 the lower reaches, the flows followed multiple channels, and broke out and branched in  
644 several places, likely due to the interaction of topographic irregularities and flow  
645 momentum.

646         Terraces form when channel erosion cuts through previously deposited material.  
647 As such, they indicate variations in the locations of erosion and deposition, but need not  
648 be caused by fluvial processes. We observed erosion of previous channel floors in several  
649 places. A clear example occurred in the large dune gully shown in Fig. 9, which  
650 developed a distinct cut-bank terrace as the channel evolved. Smaller examples were seen  
651 in non-dune gullies. Bar-like deposits were observed in many of the modified channels  
652 (Fig. 15). Like terraces, such bars are not diagnostic of flowing water, but simply indicate  
653 localized erosion and deposition by particular flows, with the gross dimensions of the  
654 gully likely set by the largest events.

655         Lobate flow deposits occur near the toes of many changes. Figure 16 shows an  
656 example formed in Istok crater (45.1°S, 274.2°E), likely in the winter of MY 33. The

657 deposit resembles features in the same crater interpreted by Johnsson et al. (2014) and de  
658 Haas et al. (2015b) as aqueous debris flows. Boulder-rich levees also formed along  
659 segments of this flow. In general, levees are uncommon (or not resolved) in current  
660 flows, but they are also uncommon in gullies as a whole. Large, leveed lobate deposits  
661 have also been observed on equatorial sand dunes, so the formation of leveed flows in  
662 general is possible at present.

663 Conway et al. (2015) suggested that various measures of concavity of the  
664 longitudinal profile of gullies were diagnostic of aqueous processes. We examined the  
665 longitudinal profile of the major dune gully in eastern Matara crater (Fig. 17) using a  
666 high-resolution Digital Terrain Model. This gully (Fig. 1f) has shown annual large-scale  
667 activity sufficient to substantially rework the morphology within a decade, so it is  
668 unlikely to preserve morphologies not produced by current processes. This gully falls  
669 within the normal range of Martian gullies for several measures of concavity (Fig. 17),  
670 demonstrating that those parameters can be produced by current CO<sub>2</sub> ice processes.

671 The massive changes observed in some dune gullies (e.g., Fig. 9) demonstrate that  
672 gullies with the classic alcove-channel-apron morphology can be swiftly created or  
673 modified by current processes. It is not plausible that such gullies preserve morphologies  
674 established during a high-obliquity ice age while many thousands of cubic meters of sand  
675 are eroded and deposited annually. Although reworking on this scale has so far only been  
676 observed in dune gullies, the differences between activity in dune and non-dune gullies  
677 appear to be in scale rather than in kind (likely because sand is not very cohesive and  
678 easily mobilized). Furthermore, current activity appears capable of initiating gullies (Fig.

679 8), not merely modifying older features. Thus, our observations show that current  
680 processes are capable of creating the classic gully morphology.

681

### 682 **A Dry Frost Model for Gully Formation and Evolution**

683         This study of Martian gully activity yields several fundamental results. First,  
684 current activity is driven by seasonal frost, which is predominantly CO<sub>2</sub>, and not by liquid  
685 water. Second, this present-day activity is extensive and could be observed in most  
686 gullies, given a sufficiently long observation period. Finally, diverse gully morphologies,  
687 including those sometimes considered diagnostic of liquid water, are forming today.  
688 Anything that does happen, can happen—and therefore, these observations demonstrate  
689 that gully formation is active, ongoing, and does not require significant volumes of liquid  
690 water. In light of these results, we propose that the fresh Martian gullies are not water-  
691 formed features, and that bulk volumes of liquid water were never present in the gullies.  
692 Instead, they form through dry, frost-driven processes.

693         In this model, individual gullies begin with events like the erosion seen in Raga  
694 crater (Fig. 8), localized by irregularities in the topography like the ill-defined partial  
695 channel at that site. Such irregularities also likely form the initiation points for alcoves.  
696 The concentration of frost activity in alcoves, combined with the locally steeper slopes,  
697 demonstrates that frost-driven processes can be concentrated within gullies in a positive  
698 feedback. Micro-topographic control of frost also enables the occurrence of ices on  
699 slopes where the overall orientation is not conducive to frost formation. Such topographic  
700 effects may control the locations of gullies, and likely explain the miscorrelations  
701 between model-predicted CO<sub>2</sub> frost and gully locations reported by Conway et al. (2016).

702 Many of these flows (tens to hundreds) build up a full-scale gully landform. The  
703 evolution is erratic, due to the variable size and erosive effects of the flows: channels  
704 form, low-energy flows result in local infill and deposition, energetic events break out to  
705 form new branches leading to channel abandonment, and sinuous curves develop and are  
706 cut off, while the alcove gradually expands. All of these phenomena have been observed  
707 and, integrated over many flows, will build the complex morphologies of well-developed  
708 gullies. The observed rate of activity in southern-hemisphere gullies implies hundreds of  
709 mass movements in individual gullies in a few Ma or less. Given the nature and extent of  
710 activity, it appears plausible for the observed gullies to form via current processes, with  
711 some variations in location and intensity over time due to climate variations, without  
712 melting or runoff. Table 1 summarizes a range of previous observations of gullies and  
713 their explanation in the seasonal frost model.

714         There is little to distinguish currently active gullies from most of those not (yet)  
715 known to be active. Dundas et al. (2015b) found that northern-hemisphere gullies were  
716 less active than those in the south, likely due to the current coincidence of aphelion and  
717 southern winter solstice, and this remains true in our larger data set. Dune gullies appear  
718 to be more active than those on non-sandy material, which likely reflects the ease of  
719 mobilizing loose sand. Degraded-appearing gullies appear less active or inactive (Dundas  
720 et al., 2015b), but it is very likely that most other gullies would show activity if  
721 monitored for decades or centuries. Certain locations like Gasa crater are particularly  
722 active at present, due to locally favorable frost conditions or especially steep or erodible  
723 material.



724 An important consequence of the frequent current activity is that it has reshaped  
725 most gullies and controls their morphology. This is most obvious in the complete  
726 reworking of large dune gullies within a decade (Fig. 9). However, there have probably  
727 been dozens or hundreds of flows in most fresh-looking gullies since the last high-  
728 obliquity period (Dundas et al., 2015b). Single flows can have significant geomorphic  
729 impacts, so the cumulative effects of many such events must have obliterated any features  
730 unique to high-obliquity conditions. In fact, an important question is why current  
731 processes have not degraded mid-latitude craters more thoroughly. There are two likely  
732 contributing factors (Dundas et al., 2015b). First, gully erosion may be most effective on  
733 steep, fresh slopes, especially at lower latitudes where slopes and shadowing are required  
734 for frost to accumulate. This would make it self-limiting as a geomorphic agent (cf. de  
735 Haas et al., 2015a). Consistent with this, the very young Gasa crater has already  
736 developed prominent gullies. (An important factor in the large Gasa crater gullies may be  
737 generation of the initial alcoves by landslides (Okubo et al., 2011), and the target  
738 materials may also be unusual (Schon and Head, 2012).) Second, mantling deposits from  
739 high-obliquity epochs fill and bury gullies, with gully erosion in many cases confined to  
740 the mantle (e.g., Christensen, 2003; Schon and Head, 2011; Aston et al., 2011; Raack et  
741 al., 2012; Conway and Balme, 2014; Dickson et al., 2015a), while erosion of bedrock  
742 alcoves occurs more slowly. This points to a model where gullies largely develop within  
743 unconsolidated material (sand and mantle deposits) and only slowly modify coherent  
744 rock. The likely formation timescale of fresh non-dune gullies by current processes is ~1–  
745 10 Ma based on rough estimation of mass fluxes (Dundas et al., 2015b). Consistent with  
746 this, upper bounds of one to several Ma have been reported for gully ages at several

747 locations (Malin and Edgett, 2000; Reiss et al., 2004; Schon et al., 2009). Such upper  
748 bounds are consistent with ongoing formation and could allow older initiation,  
749 subsequently reworked. One possibility is that the current generation of gullies began  
750 forming around the transition to lower mean obliquity thought to have occurred at ~5 Ma  
751 (Levrard et al., 2004); perhaps mid-latitude mantle deposition competed with gully  
752 erosion more effectively at higher obliquities (cf. Madeleine et al., 2014). However,  
753 current flux estimates are not precise enough to prove such a connection.

754       Climate variations are permitted by this model, and should be expected. Changes  
755 in the orbital and axial parameters (Laskar et al., 2004) must affect mid-latitude and polar  
756 ices. There is evidence for a substantial mass of CO<sub>2</sub> stored in the south polar layered  
757 deposits, capable of doubling the surface pressure if it were all added to the atmosphere  
758 (Phillips et al., 2011; Bierson et al., 2016). These factors have likely caused variations in  
759 humidity (e.g., Mischna and Richardson, 2005), ground ice stability (e.g., Mellon and  
760 Jakosky, 1995; Chamberlain and Boynton, 2007; Schorghofer and Forget, 2012), and  
761 sublimation of surface ice and deposition of frost and snow (e.g., Levrard et al., 2004;  
762 2007; Forget et al., 2006; Madeleine et al., 2009; 2014), among other variables. However,  
763 they may not have produced any significant amount of surface liquid water in the gullies.  
764 Pilorget and Forget (2016) demonstrated that the spatial distribution of CO<sub>2</sub> deposition  
765 and activity changes with obliquity. These variations, rather than variations in H<sub>2</sub>O frost  
766 and snow, could account for formation of gullies that are currently inactive and cratered  
767 (cf. Morgan et al., 2010; Raack et al., 2012).

768       Climate variations could even have produced temperatures and pressures that  
769 were commonly above the triple point of water (e.g., Dickson et al., 2015b) without

770 generating runoff. There are two reasons for this. First, latent heat loss to sublimation  
771 makes it difficult for the temperature to ever rise to the melting point if water ice is  
772 present, as discussed above. Second, there is a difference between thermodynamic  
773 stability and stability against transport. Conditions above the triple point would make  
774 liquid water thermodynamically favored if H<sub>2</sub>O were present. However, those same  
775 conditions would drive H<sub>2</sub>O away and prevent condensation, because they cause a high  
776 mean vapor pressure which makes ice (and water) unstable (e.g., Leighton and Murray,  
777 1966). Ice could be left over from cold climate conditions, but any ice transitioning  
778 towards conditions where melting temperatures might be possible would have a vapor  
779 pressure high enough to sublimate rapidly (Mellon and Phillips, 2001).

780 Counterintuitively, the existence of gullies cut into the ice-rich mid-latitude mantle is a  
781 strong argument that it has not melted—if local melting conditions were ever attained, the  
782 adjacent areas would have undergone massive losses to sublimation, destroying the  
783 mantle. The warm locations capable of exceeding the triple point are the locations where  
784 ice would be least likely to exist at all, and where ice exists, latent heat will buffer the  
785 temperature and make it difficult to reach the melting point. Some models do suggest that  
786 limited amounts of past snowmelt (few mm/year) could have occurred (Williams et al.,  
787 2009), but trace runoff typically does not produce large mass movements, while the CO<sub>2</sub>  
788 processes occurring at present clearly do so.

789         How long have such dry conditions prevailed on Mars? A generally dry climate  
790 may have prevailed for much of the Amazonian, as the atmospheric pressure has been  
791 low throughout (e.g., Lammer et al., 2013). Exceptions could have occurred in  
792 association with major transient events like impacts and volcanic eruptions. Richardson

793 and Mischna (2005) argued that the middle period of Martian history may have been even  
794 less favorable to surface liquid than the present. Recurring Slope Lineae, the other  
795 leading candidate for current near-surface liquid water flow (McEwen et al., 2011) are  
796 not understood and have angle-of-repose slopes consistent with dry granular flow  
797 (Dundas et al., 2017). Forget et al. (2013) demonstrated that formation of extensive  
798 seasonal CO<sub>2</sub> ice is a likely consequence of many ancient climate scenarios with a thicker  
799 atmosphere, particularly for an atmospheric pressure  $\leq 0.5$  bars, so dry frost processes  
800 may have occurred through most of Mars' history. However, the evidence for ancient  
801 liquid water is diverse, although the climate remains poorly understood (Wordsworth,  
802 2016). On early Mars, CO<sub>2</sub>-driven processes may have been in competition with or  
803 secondary to runoff rather than the dominant process, transitioning as the planet grew  
804 colder and drier.

805         These gully processes could be recorded in Martian sediments dating from any  
806 location and epoch with a CO<sub>2</sub> frost cycle, and this possibility should be considered in  
807 interpreting Martian sediments, particularly at middle and high latitudes. The gully mass  
808 movements transport material ranging from fine grains (including sand and airfall dust) to  
809 meter-scale boulders. The morphological similarities between CO<sub>2</sub>-driven activity and  
810 aqueous debris flows suggest that the deposits may also be similar, and CO<sub>2</sub>-mobilized  
811 flows could have fluidization similar to wet debris flows, so such deposits on Mars  
812 should not be regarded as proof of liquid water. Diagnostic differences could exist, but  
813 none of the new Martian flows has yet been inspected in situ for comparison. (At the time  
814 of writing, the *Opportunity* rover is preparing to investigate a degraded gully-like feature  
815 in Meridiani Planum (Parker et al., 2017). The feature is poorly developed compared

816 with many mid-latitude gullies, and the equatorial latitude (2.3°S) is less favorable for  
817 past CO<sub>2</sub> processes, but CO<sub>2</sub>-driven formation should be considered a possible working  
818 hypothesis.) The most likely difference between aqueous and CO<sub>2</sub>-driven mass  
819 movements is possible evidence for loss of ice that was mixed into the final deposit and  
820 later sublimated, which could manifest as voids or larger collapse or fluidization features,  
821 but the absence of such features would not necessarily rule out CO<sub>2</sub> frost. Sediments with  
822 evidence for sustained flow and deposition, such as bedform migration, are much more  
823 likely to be fluvial (or aeolian), although the deposition style of slowly creeping  
824 defrosting flows is unknown. Dune gully flows, if preserved in ancient sandstone, are  
825 presumably entirely sand, and linear-gully pits formed by sublimating blocks (Diniaga et  
826 al., 2013) would disrupt existing bedding.

827         We emphasize several key points for further assessment of this hypothesis.  
828 Current Martian processes are carving sinuous channels, creating lobate flows, and  
829 producing other morphologies resembling water-formed terrestrial features. Arguments  
830 that particular liquid-free processes on Earth do not produce these morphologies are not  
831 convincing tests. Unless large volumes of liquid water are being regularly generated in  
832 individual gullies by some unknown mechanism and preferentially released in winter,  
833 some non-aqueous process is capable of making these features under Martian conditions.  
834 As we do not have terrestrial analogs for gullies formed by CO<sub>2</sub> frost, we do not know  
835 what their morphology and morphometry “should” be. The current formation of aqueous-  
836 like landforms on Mars suggests that they would resemble water-formed terrestrial  
837 features. It is difficult to categorically prove that runoff during some past high-obliquity  
838 climate did not contribute to gully formation, and we do not rule out the possibility of

839 some surface liquid water in the geologically recent past. However, the essential  
840 argument for liquid water carving gullies is that their morphology is uniquely water-  
841 formed and has survived since the last period of high axial tilt. The nature and frequency  
842 of current activity in fresh gullies make that interpretation difficult to sustain.

843

#### 844 **Conclusions**

845 Extensive activity is occurring in Martian gullies today, including formation of a  
846 host of geomorphic features often associated with water. However, the timing of activity,  
847 and the dry Martian climate, indicate that seasonal CO<sub>2</sub> frost is the cause. The flows seen  
848 within Martian gullies may resemble those produced by aqueous processes because they  
849 are fluidized to some extent, likely by gas generated from entrained CO<sub>2</sub> frost. Changes  
850 in gullies have significant geomorphic effects on all parts of the gully system. The  
851 extensive changes observed have likely erased and reworked any morphologies within  
852 these same gullies that formed during the last high-obliquity period, so gully  
853 geomorphology cannot be diagnostic of liquid water occurring only in a past climate.  
854 HiRISE observations indicate that Martian gullies are forming today. Liquid water is not  
855 necessary for the gullies, and may never have been involved in their formation. Such a  
856 dry scenario would mean that gullies need not be treated as potential naturally-occurring  
857 Special Regions, although the likely presence of shallow water ice on pole-facing slopes  
858 in the mid-latitudes would still make them potential induced Special Regions. CO<sub>2</sub> frost  
859 processes have likely been active for much of Mars' geologic history, with geomorphic  
860 and sedimentary consequences that are not yet understood.

861

862 **Acknowledgments**

863           This work was funded by Mars Data Analysis Program grant NNH13AV85I and  
864 the Mars Reconnaissance Orbiter HiRISE project. SD's work was carried out at the Jet  
865 Propulsion Laboratory, California Institute of Technology, under a contract with the  
866 National Aeronautics and Space Administration (NASA). We thank the HiRISE  
867 operations team for acquiring and processing the data, the MRO CTX team for  
868 suggesting some locations of possible activity for HiRISE imaging, and NASA for  
869 supporting the extended missions necessary to collect long-term monitoring observations.  
870 Two reviewers provided helpful comments. All HiRISE images used in this study are  
871 available via the Planetary Data System. Any use of trade, firm, or product names is for  
872 descriptive purposes only and does not imply endorsement by the U.S. Government.

873

874 **Supplementary Materials**

875           Supporting materials for this article include a description and captions for the  
876 supplementary materials, Supplementary Figures 1–6, Supplementary Animations 1–3 (as  
877 separate files), and Supplementary Tables 1–2 (as separate files).

878

879 **References**

880 Aston, A. H., Conway, S. J., Balme, M. R., 2011. Identifying Martian gully evolution. In  
881 Martian Geomorphology (Balme, M. R., Bargery, A. S., Gallagher, C. J., & Gupta, S.,  
882 eds.), Geological Society, London, Special Publication 356, 151-169,  
883 doi:10.1144/SP356.9.

884 Auld, K. S., Dixon, J. C., 2016. A classification of Martian gullies from HiRISE imagery.  
885 Planet. Space Sci., 131, 88-101, doi:10.1016/j.pss.2016.08.002.

886 Ayoub, F., Avouac, J.-P., Newman, C. E., Richardson, M. I., Lucas, A., Leprince, S.,  
887 Bridges, N. T., 2014. Threshold for sand mobility on Mars calibrated from seasonal  
888 variations of sand flux. Nature Commun., 5:5096, doi:10.1038/ncomms6096.

889 Balme, M., Mangold, N., Baratoux, D., Costard, F., Gosselin, F., Masson, P., Pinet, P.,  
890 Neukum, G., 2006. Orientation and distribution of recent gullies in the southern  
891 hemisphere of Mars: Observations from High Resolution Stereo Camera/Mars  
892 Express (HRSC/MEX) and Mars Orbiter Camera/Mars Global Surveyor  
893 (MOC/MGS) data. J. Geophys. Res., 111, E05001, doi:10.1029/2005JE002607.

894 Bart, G. D., 2007. Comparison of small lunar landslides and Martian gullies. Icarus, 187,  
895 417-421, doi:10.1016/j.icarus.2006.11.004.

896 Bierson, C. J., Phillips, R. J., Smith, I. B., Wood, S. E., Putzig, N. E., Nunes, D., Byrne,  
897 S., 2016. Stratigraphy and evolution of the buried CO<sub>2</sub> deposit in the Martian south  
898 polar cap. Geophys. Res. Lett., 43, doi:10.1002/2016GL068457.

899 Branney, M. J., Kokelaar, P., 2002. Pyroclastic density currents and the sedimentation of  
900 ignimbrites. Geol. Soc. Memoir No. 27, Geological Society, London, 152 pp.

901 Bridges, N.T., Lackner, C.N., 2006. Northern hemisphere Martian gullies and mantled  
902 terrain: Implications for near-surface water migration in Mars' recent past. J.  
903 Geophys. Res., 111, E09014, doi:10.1029/2006JE002702.

904 Bridges, N.T., Herkenhoff, K.E., Titus, T.N., Kieffer, H.H., 2001. Ephemeral dark spots  
905 associated with Martian gullies. Lunar Planet. Sci. Conf. 32, abstract #2126.

906 Carr, M. H., 2006. The Surface of Mars. Cambridge University Press, Cambridge, 307 p.



907 Cedillo-Flores, Y., Treiman, A. H., Lasue, J., Clifford, S. M., 2011. CO<sub>2</sub> gas fluidization  
908 in the initiation and formation of Martian polar gullies. *Geophys. Res. Lett.*, 38,  
909 L21202, doi:10.1029/2011GL049403.

910 Chamberlain, M. A., Boynton, W. V., 2007. Response of Martian ground ice to orbit-  
911 induced climate change. *J. Geophys. Res.*, 112, E06009, doi:10.1029/2006JE002801.

912 Christensen, P.R., 2003. Formation of recent Martian gullies through melting of extensive  
913 water-rich snow deposits. *Nature*, 422, 45-48, doi:10.1038/nature01436.

914 Clancy, R.T., Sandor, B.J., Wolff, M.J., Christensen, P.R., Smith, M.D., Pearl, J.C.,  
915 Conrath, B.J., Wilson, R.J., 2000. An intercomparison of groundbased millimeter,  
916 MGS TES, and Viking atmospheric temperature measurements: Seasonal and  
917 interannual variability of temperatures and dust loading in the global Mars  
918 atmosphere. *J. Geophys. Res.*, 105, 9553–9572, doi:10.1029/1999JE001089.

919 Conway, S. J., Balme, M. R., 2014. Decameter thick remnant glacial ice deposits on  
920 Mars. *Geophys. Res. Lett.*, 41, 5402-5409, doi:10.1002/2014GL060314.

921 Conway, S. J., Balme, M. R., 2016. A novel topographic parameterization scheme  
922 indicates that Martian gullies display the signature of liquid water. *Earth Planet. Sci.*  
923 *Lett.*, 454, 36-45, doi:10.1016/j.epsl.2016.08.031.

924 Conway, S. J., Balme, M. R., Kreslavsky, M. A., Murray, J. B., Towner, M. C., 2015.  
925 The comparison of topographic long profiles of gullies on Earth to gullies on Mars: A  
926 signal of water on Mars. *Icarus*, 253, 189-204, doi:10.1016/j.icarus.2015.03.009.

927 Conway, S. J., Harrison, T. N., Lewis, S. R., Soare, R. J., Balme, M. R., Britton, A.,  
928 2016. Martian gully orientation and slope used to test meltwater and carbon dioxide  
929 hypotheses. *Lunar Planet. Sci. Conf. 47*, abstract #1973.

930 Costard, F., Forget, F., Mangold, N., Peulvast, J.P., 2002. Formation of recent Martian  
931 debris flows by melting of near-surface ground ice at high obliquity. *Science*, 295,  
932 110–113, doi:10.1126/science.1066698.

933 de Haas, T., Hauber, E., Kleinhans, M. G., 2013. Local late Amazonian boulder  
934 breakdown and denudation rate on Mars. *Geophys. Res. Lett.*, 40, 3527-3531,  
935 doi:10.1002/grl.50726.

936 de Haas, T., Conway, S. J., Krautblatter, M., 2015a. Recent (Late Amazonian) enhanced  
937 backweathering rates on Mars: Paracratering evidence from gully alcoves. *J.*  
938 *Geophys. Res. Planets*, 120, doi:10.1002/2015JE004915.

939 de Haas, T., Hauber, E., Conway, S. J., van Steijn, H., Johnsson, A., Kleinhans, M. G.,  
940 2015b. Earth-like aqueous debris-flow activity on Mars at high orbital obliquity in the  
941 last million years. *Nature Commun.*, 6:7543, doi:10.1038/ncomms8543.

942 de Haas, T., Ventra, D., Hauber, E., Conway, S. J., Kleinhans, M. G., 2015c.  
943 Sedimentological analyses of Martian gullies: The subsurface as the key to the  
944 surface. *Icarus*, 258, 92-108, doi:10.1016/j.icarus.2015.06.017.

945 Delamere, W. A., et al., 2010. Color imaging of Mars by the High Resolution Imaging  
946 Science Experiment (HiRISE). *Icarus*, 205, 38-52, doi:10.1016/j.icarus.2009.03.012.

947 Dickson, J. L. Head, J.W., 2009. The formation and evolution of youthful gullies on  
948 Mars: Gullies as the late-stage phase of Mars' most recent ice age. *Icarus*, 204, 63-86,  
949 doi:10.1016/j.icarus.2009.06.018.

950 Dickson, J. L., Head, J.W., Kreslavsky, M., 2007. Martian gullies in the southern mid-  
951 latitudes of Mars: Evidence for climate-controlled formation of young fluvial features

952 based upon local and global topography. *Icarus*, 188, 315-323,  
953 doi:10.1016/j.icarus.2006.11.020.

954 Dickson, J. L., Head, J. W., Goudge, T. A., Barbieri, L., 2015a. Recent climate cycles on  
955 Mars: Stratigraphic relationships between multiple generations of gullies and the  
956 latitude-dependent mantle. *Icarus*, 252, 83-94, doi:10.1016/j.icarus.2014.12.035.

957 Dickson, J. L., Kerber, L., Fassett, C. I., Head, J. W., Forget, F., Madeleine, J.-B., 2015b.  
958 Formation of gullies on Mars by water at high obliquity: Quantitative integration of  
959 Global Climate Models and gully distribution. *Lunar Planet. Sci. Conf.* 46, abstract  
960 #1035.

961 Diniega, S., Byrne, S., Bridges, N.T., Dundas, C.M., McEwen, A.S., 2010. Seasonality of  
962 present-day Martian dune-gully activity. *Geology*, 38, 1047-1050,  
963 doi:10.1130/G31287.1.

964 Diniega, S., Hansen, C.J., McElwaine, J.N., Hugenholtz, C.H., Dundas, C.M., McEwen,  
965 A.S., Bourke, M.C., 2013. A new dry hypothesis for the formation of Martian linear  
966 gullies. *Icarus*, 225, 526-537, doi:10.1016/j.icarus.2013.04.006.

967 Dundas, C. M., Byrne, S., 2010. Modeling sublimation of ice exposed by new impacts in  
968 the Martian mid-latitudes. *Icarus*, 206, 716-728, doi:10.1016/j.icarus.2009.09.007.

969 Dundas, C.M., McEwen, A.S., Diniega, S., Byrne, S., Martinez-Alonso, S., 2010. New  
970 and recent gully activity on Mars as seen by HiRISE. *Geophys. Res. Lett.*, 37,  
971 L07202, doi:10.1029/2009GL041351.

972 Dundas, C.M., Diniega, S., Hansen, C.J., Byrne, S., McEwen, A.S., 2012. Seasonal  
973 activity and morphological changes in Martian gullies. *Icarus*, 220, 124-143,  
974 doi:10.1016/j.icarus.2012.04.005.

975 Dundas, C. M., Byrne, S., McEwen, A. S., 2015a. Modeling the development of Martian  
976 sublimation thermokarst landforms. *Icarus*, 262, 154-169,  
977 doi:10.1016/j.icarus.2015.07.033.

978 Dundas, C.M., Diniega, S., McEwen, A.S., 2015b. Long-term monitoring of Martian  
979 gully formation and evolution with MRO/HiRISE. *Icarus*, 251, 244-263,  
980 doi:10.1016/j.icarus.2014.05.013.

981 Dundas, C. M., McEwen, A. S., Chojnacki, M., Milazzo, M. P., Byrne, S., 2017. A  
982 granular flow model for Recurring Slope Lineae on Mars. *Lunar Planet. Sci. Conf.*  
983 48, abstract #2399.

984 Forget, F., Haberle, R. M., Montmessin, F., Levrard, B., Head, J. W., 2006. Formation of  
985 glaciers on Mars by atmospheric precipitation at high obliquity. *Science*, 311, 368-  
986 371, doi:10.1126/science.1120335.

987 Forget, F., Wordsworth, R., Millour, E., Madeleine, J.-B., Kerber, L., Leconte, J., Marcq,  
988 E., Haberle, R. M., 2013. 3D modelling of the early Martian climate under a denser  
989 CO<sub>2</sub> atmosphere: Temperatures and CO<sub>2</sub> ice clouds. *Icarus*, 222, 81-99,  
990 doi:10.1016/j.icarus.2012.10.019.

991 Forget, F., Pilorget, C., Pottier, A., Meslin, P.-Y., 2016. Deep incision of the Latitude  
992 Dependent Mantle in Martian gullies formed by CO<sub>2</sub> sublimation processes.  
993 Unnumbered abstract presented at the Workshop on Martian Gullies and their Earth  
994 Analogs, June 20, 2016, London, UK.

995 Gaidos, E.J., 2001. Cryovolcanism and the recent flow of liquid water on Mars. *Icarus*,  
996 153, 218-223, doi:10.1006/icar.2001.6649.

997 Gallagher, C., Balme, M. R., Conway, S. J., Grindrod, P. M., 2011. Sorted clastic stripes,  
998 lobes and associated gullies in high-latitude craters on Mars: Landforms indicative of  
999 very recent, polycyclic ground-ice thaw and liquid flows. *Icarus*, 211, 458-471,  
1000 doi:10.1016/j.icarus.2010.09.010.

1001 Gilmore, M. S., Phillips, E. L., 2002. Role of aquicludes in formation of Martian gullies.  
1002 *Geology*, 30, 1107-1110, doi:10.1130/0091-  
1003 7613(2002)030<1107:ROAIFO>2.0.CO;2.

1004 Goldspiel, J. M., Squyres, S. W., 2011. Groundwater discharge and gully formation on  
1005 Martian slopes. *Icarus*, 211, 238-258, doi:10.1016/j.icarus.2010.10.008.

1006 Gough, R. V., Chevrier, V. F., Baustian, K. J., Wise, M. E., Tolbert, M. A., 2011.  
1007 Laboratory studies of perchlorate phase transitions: Support for metastable aqueous  
1008 perchlorate solutions on Mars. *Earth Planet. Sci. Lett.*, 312, 371-377,  
1009 doi:10.1016/j.epsl.2011.10.026.

1010 Hansen, C. J., Okubo, C., McEwen, A., Byrne, S., DeJong, E., Herkenhoff, K., Mellon,  
1011 M., Russell, P., Thomas, N., 2007. HiRISE views of the sublimation of Mars'  
1012 southern seasonal cap. 7<sup>th</sup> Int. Conf. Mars, abstract #3364.

1013 Hansen, C. J., Thomas, N., Portyankina, G., McEwen, A., Becker, T., Byrne, S.,  
1014 Herkenhoff, K., Kieffer, H., Mellon, M., 2010. HiRISE observations of gas  
1015 sublimation-driven activity in Mars' southern polar regions: I. Erosion of the surface.  
1016 *Icarus*, 205, 283-295, doi:10.1016/j.icarus.2009.07.021.

1017 Hansen, C. J., Diniega, S., Bridges, N., Byrne, S., Dundas, C., McEwen, A., Portyankina,  
1018 G., 2015. Agents of change on Mars' northern dunes: CO<sub>2</sub> ice and wind. *Icarus*, 251,  
1019 264-274, doi:10.1016/j.icarus.2014.11.015.

1020 Harrison, T.N., 2016. Martian gully formation and evolution: Studies from the local to  
1021 global scale. Ph.D. Dissertation, Western University.

1022 Harrison, T.N., Malin, M.C., Edgett, K.S., 2009. Liquid water on the surface of Mars  
1023 today: Present gully activity observed by the Mars Reconnaissance Orbiter (MRO)  
1024 and Mars Global Surveyor (MGS) and direction for future missions. AGU Fall  
1025 Meeting, abstract #P43D-1454.

1026 Harrison, T. N., Osinski, G. R., Tornabene, L. L., Jones, E., 2015. Global documentation  
1027 of gullies with the Mars Reconnaissance Orbiter Context Camera and implications for  
1028 their formation. *Icarus*, 252, 236-254, doi:10.1016/j.icarus.2015.01.022.

1029 Hartmann, W.K., 2001. Martian seeps and their relation to youthful geothermal activity.  
1030 *Space Sci. Rev.*, 96, 405-410.

1031 Hartmann, W. K., Thorsteinsson, T., Sigurdsson, F., 2003. Martian hillside gullies and  
1032 Icelandic analogs. *Icarus*, 162, 259-277, doi:10.1016/S0019-1035(02)00065-9.

1033 Hayne, P. O., Paige, D. A., Heavens, N. G., and the Mars Climate Sounder Science  
1034 Team, 2014. The role of snowfall in forming the seasonal ice caps of Mars: Models  
1035 and constraints from the Mars Climate Sounder. *Icarus*, 231, 122-130,  
1036 doi:10.1016/j.icarus.2013.10.020.

1037 Hecht, M.H., 2002. Metastability of liquid water on Mars. *Icarus*, 156, 373-386,  
1038 doi:10.1006/icar.2001.6794.

1039 Heldmann, J. L., Mellon, M. T., 2004. Observations of Martian gullies and constraints on  
1040 potential formation mechanisms. *Icarus*, 168, 285-304,  
1041 doi:10.1016/j.icarus.2003.11.024.

1042 Heldmann, J.L., Carlsson, E., Johansson, H., Mellon, M.T., Toon, O.B., 2007.  
1043 Observations of Martian gullies and constraints on potential formation mechanisms:  
1044 II. The northern hemisphere. *Icarus*, 188, 324–344, doi:10.1016/j.icarus.2006.12.010.  
1045 Hoffman, N., 2002. Active polar gullies on Mars and the role of carbon dioxide.  
1046 *Astrobiology*, 2, 313–323, doi:10.1089/153110702762027899.  
1047 Hugenholtz, C.H., 2008. Frosted granular flow: A new hypothesis for mass wasting in  
1048 Martian gullies. *Icarus* 197, 65–72, doi:10.1016/j.icarus.2008.04.010.  
1049 Ingersoll, A., 1970. Mars: Occurrence of liquid water. *Science*, 168, 972-973,  
1050 doi:10.1126/science.168.3934.972.  
1051 Ishii, T., Sasaki, S., 2004. Formation of recent Martian gullies by avalanches of CO<sub>2</sub>  
1052 Frost. *Lunar Planet. Sci. Conf.* 35, abstract #1556.  
1053 Ishii, T., Miyamoto, H., Sasaki, S., Tajika, E., 2006. Constraints on the formation of  
1054 gullies on Mars: A possibility of the formation of gullies by avalanches of granular  
1055 CO<sub>2</sub> ice particles. *Lunar Planet. Sci. Conf.* 37, abstract #1646.  
1056 Iverson, R. M., 1997. The physics of debris flows. *Rev. Geophys.*, 35, 245-296,  
1057 doi:10.1029/97RG00426.  
1058 Johnsson, A., Reiss, D., Hauber, E., Hiesinger, H., Zanetti, M., 2014. Evidence for very  
1059 recent melt-water and debris flow activity in gullies in a young mid-latitude crater on  
1060 Mars. *Icarus*, 235, 37-54, doi:10.1016/j.icarus.2014.03.005.  
1061 Kieffer, H. H., 2000. Annual punctuated CO<sub>2</sub> slab-ice and jets on Mars. *Mars Polar Sci.*  
1062 *Conf.*, abstract #4095.  
1063 Kieffer, H. H., 2007. Cold jets in the Martian polar caps. *J. Geophys. Res.*, 112, E08005,  
1064 doi:10.1029/2006JE002816.

1065 Knauth, L. P., Burt, D. M., 2002. Eutectic brines on Mars: Origin and possible relation to  
1066 young surface features. *Icarus*, 158, 267-271, doi:10.1006/icar.2002.6866.

1067 Kneissl, T., Reiss, D., van Gasselt, S., Neukum, G., 2010. Distribution and orientation of  
1068 northern-hemisphere gullies on Mars from the evaluation of HRSC and MOC-NA  
1069 data. *Earth Planet. Sci. Lett.*, 294, 357-367, doi:10.1016/j.epsl.2009.05.018.

1070 Kolb, K.J., Pelletier, J.D., McEwen, A.S., 2010a. Modeling the formation of bright slope  
1071 deposits associated with gullies in Hale crater, Mars: Implications for recent liquid  
1072 water. *Icarus*, 205, 113-137, doi:10.1016/j.icarus.2009.09.009.

1073 Kolb, K.J., Pelletier, J.D., McEwen, A.S., 2010b. Investigating gully flow emplacement  
1074 mechanisms using apex slopes. *Icarus*, 208, 132-142,  
1075 doi:10.1016/j.icarus.2010.01.007.

1076 Kossacki, K.J., Markiewicz, W.J., 2004. Seasonal melting of surface water ice  
1077 condensing in Martian gullies. *Icarus*, 171, 272-283,  
1078 doi:10.1016/j.icarus.2004.05.018.

1079 Kumar, P. S., Keerthi, V., Kumar, A. S., Mustard, J., Krishna, B. G., Amitabh, Ostrach,  
1080 L. R., Kring, D. A., Kumar, A. S. K., Goswami, J. N., 2013. Gullies and landslides on  
1081 the Moon: Evidence for dry-granular flows. *J. Geophys. Res.*, 118,  
1082 doi:10.1002/jgre.20043.

1083 Lammer, H., Chassefière, E., Karatekin, O., Morschhauser, A., Niles, P. B., Mousis, O.,  
1084 Odert, P., Möstl, U. V., Breuer, D., Dehant, V., Grott, M., Gröller, H., Hauber, E.,  
1085 Pham, L. B. S., 2013. Outgassing history and escape of the Martian atmosphere and  
1086 water inventory. *Space Sci. Rev.*, 174, 113-154, doi:10.1007/s11214-012-9943-8.



1087 Lanza, N. L., Meyer, G. A., Okubo, C. H., Newsom, H. E., Wiens, R. C., 2010. Evidence  
1088 for debris flow gully formation initiated by shallow subsurface water on Mars. *Icarus*,  
1089 205, 103-112, doi:10.1016/j.icarus.2009.04.014.

1090 Laskar, J., Correia, A.C.M., Gastineau, M., Joutel, F., Levrard, B., Robutel, P., 2004.  
1091 Long term evolution and chaotic diffusion of the insolation quantities of Mars. *Icarus*,  
1092 170, 343-364, doi:10.1016/j.icarus.2004.04.005.

1093 Lee, P., Cockell, C. S., Marinova, M. M., McKay, C. P., Rice, J. W., 2001. Snow and ice  
1094 melt flow features on Devon Island, Nunavut, Arctic Canada as possible analogs for  
1095 recent slope flow features on Mars. *Lunar Planet. Sci. Conf. 32*, abstract #1809.

1096 Leighton, R. B., Murray, B. C., 1966. Behavior of carbon dioxide and other volatiles on  
1097 Mars. *Science*, 153, 136-144, doi:10.1126/science.153.3732.136.

1098 Levrard, B., Forget, F., Montmessin, F., Laskar, J., 2004. Recent ice-rich deposits formed  
1099 at high latitudes on Mars by sublimation of unstable equatorial ice during low  
1100 obliquity. *Nature*, 431, 1072-1075, doi:10.1038/nature03055.

1101 Levrard, B., Forget, F., Montmessin, F., Laskar, J., 2007. Recent formation and evolution  
1102 of northern Martian polar layered deposits as inferred from a Global Climate Model.  
1103 *J. Geophys. Res.*, 112, E06012, doi:10.1029/2006JE002772.

1104 Levy, J. S., Head, J. W., Dickson, J. L., Fassett, C. I., Morgan, G. A., Schon, S. C., 2010.  
1105 Identification of gully debris flow deposits in Protonilus Mensae, Mars:  
1106 Characterization of a water-bearing, energetic gully-forming process. *Earth Planet.*  
1107 *Sci. Lett.*, 294, 368-377, doi:10.1016/j.epsl.2009.08.002.

1108 Madeleine, J.-B., Forget, F., Head, J. W., Levrard, B., Montmessin, F., Millour, E., 2009.  
1109 Amazonian northern mid-latitude glaciation on Mars: A proposed climate scenario.  
1110 Icarus, 203, 390-405, doi:10.1016/j.icarus.2009.04.037.

1111 Madeleine, J.-B., Head, J. W., Forget, F., Navarro, T., Millour, E., Spiga, A., Colaïtis, A.,  
1112 Määttänen, A., Montmessin, F., Dickson, J. L., 2014. Recent Ice Ages on Mars: The  
1113 role of radiatively active clouds and cloud microphysics. Geophys. Res. Lett., 41,  
1114 4873-4879, doi:10.1002/2014GL059861.

1115 Malin, M.C., Edgett, K.S., 2000. Evidence for recent groundwater seepage and surface  
1116 runoff on Mars. Science, 288, 2330-2335, doi:10.1126/science.288.5475.2330.

1117 Malin, M. C., Edgett, K. S., 2005. 8 years at Mars #1: New dune gullies, Malin Space  
1118 Science Systems captioned image release, MOC2-1220, NASA/JPL Planetary  
1119 Photojournal, <http://photojournal.jpl.nasa.gov/>, catalog number PIA04290.

1120 Malin, M.C., Edgett, K.S., Posiolova, L.V., McColley, S.M., Dobrea, E.Z.N., 2006.  
1121 Present-day impact cratering rate and contemporary gully activity on Mars. Science,  
1122 314, 1573–1577, doi:10.1126/science.1135156.

1123 Mangold, N., Costard, F., 2003. Debris flows over sand dunes on Mars: Evidence for  
1124 liquid water. J. Geophys. Res., 108, 5027, doi:10.1029/2002JE001958.

1125 Mangold, N., Baratoux, D., Costard, F., Forget, F., 2008. Current gullies activity: Dry  
1126 avalanches observed over seasonal frost as seen on HiRISE images. Workshop on  
1127 Martian gullies: Theories and Tests, abstract #8005.

1128 Mangold, N., Mangeney, A., Migeon, V., Ansan, V., Lucas, A., Baratoux, D., Bouchut,  
1129 F., 2010. Sinuous gullies on Mars: Frequency, distribution, and implications for flow  
1130 properties. J. Geophys. Res., 115, E11001, doi:10.1029/2009JE003540.

1131 Massé, M., Conway, S. J., Gargani, J., Patel, M. R., Pasquon, K., McEwen, A., Carpy, S.,  
1132 Chevrier, V., Balme, M. R., Ojha, L., Vincendon, M., Poulet, F., Costard, F.,  
1133 Jouannic, G., 2016. Transport processes induced by metastable boiling water under  
1134 Martian surface conditions. *Nature Geosci.*, 9, 425-428, doi:10.1038/NGEO2706.

1135 McEwen, A.S., Eliason, E.M., Bergstrom, J.W., Bridges, N.T., Hansen, C.J., Delamere,  
1136 W.A., Grant, J.A., Gulick, V.C., Herkenhoff, K.E., Keszthelyi, L., Kirk, R.L., Mellon,  
1137 M.T., Squyres, S.W., Thomas, N., Weitz, C.M., 2007a. Mars Reconnaissance  
1138 Orbiter's High Resolution Imaging Science Experiment (HiRISE). *J. Geophys. Res.*,  
1139 112, E05S02, doi:10.1029/2005JE002605.

1140 McEwen, A. S., Ojha, L., Dundas, C. M., Mattson, S. S., Byrne, S., Wray, J. J., Cull, S.  
1141 C., Murchie, S. L., Thomas, N., Gulick, V. C., 2011. Seasonal flows on warm Martian  
1142 slopes. *Science*, 333, 740-743, doi:10.1126/science.1204816.

1143 McEwen, A. S., Dundas, C. M., Mattson, S. S., Toigo, A. D., Ojha, L., Wray, J. J.,  
1144 Chojnacki, M., Byrne, S., Murchie, S. L., Thomas, N., 2014. Recurring slope lineae  
1145 in equatorial regions of Mars. *Nat. Geosci.*, 7, 53-58, doi:10.1038/ngeo2014.

1146 McEwen, A. S., Dundas, C. M., Chojnacki, M., Massé, M., 2016. Small Martian gullies  
1147 associated with Recurring Slope Lineae. Unnumbered abstract presented at the  
1148 Workshop on Martian Gullies and their Earth Analogs, June 20, 2016, London, UK.

1149 Mellon, M. T., Jakosky, B. A., 1995. The distribution and behavior of Martian ground ice  
1150 during past and present epochs. *J. Geophys. Res.*, 100, 11781-11799,  
1151 doi:10.1029/95JE01027.

1152 Mellon, M.T., Phillips, R.J., 2001. Recent gullies on Mars and the source of liquid water.  
1153 *J. Geophys. Res.*, 106, 23,165-23,180, doi:10.1029/2000JE001424.

1154 Morgan, G. A., Head, J. W., Forget, F., Madeleine, J.-B., Spiga, A., 2010. Gully  
1155 formation on Mars: Two recent phases of formation suggested by links between  
1156 morphology, slope orientation and insolation history. *Icarus*, 208, 658-666,  
1157 doi:10.1016/j.icarus.2010.02.019.

1158 Musselwhite, D.S., Swindle, T.D., Lunine, J.I., 2001. Liquid CO<sub>2</sub> breakout and the  
1159 formation of recent small gullies on Mars. *Geophys. Res. Lett.*, 28, 1283-1285,  
1160 doi:10.1029/2000GL012496.

1161 Neuendorf, K.K.E., Mehl, J.P., Jackson, J.A. (eds.), 2005. *Glossary of Geology*, 5<sup>th</sup>  
1162 Edition, American Geological Institute, 779 pp.

1163 Núñez, J. I., Barnouin, O. S., Murchie, S. L., Seelos, F. P., McGovern, J. A., Seelos, K.  
1164 D., Buczkowski, D. L., 2016. New insights into gully formation on Mars: Constraints  
1165 from composition as seen by MRO/CRISM. *Geophys. Res. Lett.*, 43, 8893-8902,  
1166 doi:10.1002/2016GL068956

1167 Okubo, C. H., Tornabene, L. L., Lanza, N. L., 2011. Constraints on mechanisms for the  
1168 growth of gully alcoves in Gasa crater, Mars, from two-dimensional stability  
1169 assessments of rock slopes. *Icarus*, 211, 207-221, doi:10.1016/j.icarus.2010.09.025.

1170 Parker, T. J., Golombek, M. P., Lamb, M., Palucis, M. C., Athena Science Team, 2017.  
1171 An opportunity to inspect a Martian gully up close. *Lunar Planet. Sci. Conf.* 48,  
1172 abstract #2468.

1173 Pasquon, K., Gargani, J., Massé, M., Conway, S. J., 2016. Present-day formation and  
1174 seasonal evolution of linear dune gullies on Mars. *Icarus*, 274, 195-210,  
1175 doi:10.1016/j.icarus.2016.03.024.

1176 Pelletier, J.D., Kolb, K.J., Kirk, R.L., 2008. Recent bright gully deposits on Mars: Wet or  
1177 dry flow? *Geology*, 36, 211–214, doi:10.1130/G24346A.1.

1178 Phillips, R.J., Davis, B.J., Tanaka, K.L., Byrne, S., Mellon, M.T., Putzig, N.E., Haberle,  
1179 R.M., Kahre, M.A., Campbell, B.C., Carter, L.M., Smith, I.B., Holt, J.W., Smrekar,  
1180 S.E., Nunes, D.C., Plaut, J.J., Egan, A.F., Titus, T.N., Seu, R., 2011. Massive CO<sub>2</sub> ice  
1181 deposits sequestered in the South Polar Layered Deposits of Mars. *Science*, 332, 838-  
1182 841, doi:10.1126/science.1203091.

1183 Pilorget, C., Forget, F., 2016. Formation of gullies on Mars by debris flows triggered by  
1184 CO<sub>2</sub> sublimation. *Nature Geosci.*, 9, 65-69, doi:10.1038/ngeo2619.

1185 Piqueux, S., Byrne, S., Richardson, M. I., 2003. Sublimation of Mars's southern seasonal  
1186 CO<sub>2</sub> ice cap and the formation of spiders. *J. Geophys. Res.*, 108,  
1187 doi:10.1029/2002JE002007.

1188 Piqueux, S., Kleinböhl, A., Hayne, P. O., Kass, D. M., Schofield, J. T., McCleese, D. J.,  
1189 2015. Variability of the Martian seasonal CO<sub>2</sub> cap extent over eight Mars Years.  
1190 *Icarus*, 251, 164-180, doi:10.1016/j.icarus.2014.10.045.

1191 Piqueux, S., Kleinböhl, A., Hayne, P. O., Heavens, N. G., Kass, D. M., McCleese, D. J.,  
1192 Schofield, J. T., Shirley, J. H., 2016. Discovery of a widespread low-latitude diurnal  
1193 CO<sub>2</sub> frost cycle on Mars. *J. Geophys. Res. Planets*, 121, doi:10.1002/2016JE005034.

1194 Raack, J., Reiss, D., Hiesinger, H., 2012. Gullies and their relationships to the dust-ice  
1195 mantle in the northwestern Argyre Basin, Mars. *Icarus*, 219, 129-141,  
1196 doi:10.1016/j.icarus.2012.02.025.

1197 Raack, J., Reiss, D., Appéré, T., Vincendon, M., Ruesch, O., Hiesinger, H., 2015.  
1198 Present-day seasonal gully activity in a south polar pit (Sisyphi Cavi) on Mars. *Icarus*,  
1199 251, 226-243, doi:10.1016/j.icarus.2014.03.040.

1200 Reiss, D., Jaumann, R., 2003. Recent debris flows on Mars: Seasonal observations of the  
1201 Russell Crater dune field. *Geophys. Res. Lett.*, 30, doi:10.1029/2002GL016704.

1202 Reiss, D., van Gasselt, S., Neukum, G., Jaumann, R., 2004. Absolute dune ages and  
1203 implications for the time of formation of gullies in Nirgal Vallis, Mars. *J. Geophys.*  
1204 *Res.*, 109, doi:10.1029/2004JE002251.

1205 Reiss, D., Erkeling, G., Bauch, K.E., Hiesinger, H., 2010. Evidence for present day gully  
1206 activity on the Russell crater dune field, Mars. *Geophys. Res. Lett.*, 37, L06203,  
1207 doi:10.1029/2009GL042192.

1208 Richardson, M. I., Mischna, M. A., 2005. Long-term evolution of transient liquid water  
1209 on Mars. *J. Geophys. Res.*, 110, E03003, doi:10.1029/2004JE002367.

1210 Rummel, J. D., and 24 coauthors, 2014. A new analysis of Mars “Special Regions”:  
1211 Findings of the Second MEPAG Special Regions Science Analysis Group (SR-  
1212 SAG2). *Astrobiology*, 14, 887-968, doi:10.1089/ast.2014.1227.

1213 Schon, S. C., Head, J. W., 2009. Terraced cutbanks and longitudinal bars in gully  
1214 channels on Mars: Evidence for multiple episodes of fluvial transport. *Lunar Planet.*  
1215 *Sci. Conf.* 40, abstract #1691.

1216 Schon, S. C., Head, J. W., 2011. Keys to gully formation processes on Mars: Relation to  
1217 climate cycles and sources of meltwater. *Icarus*, 213, 428-432,  
1218 doi:10.1016/j.icarus.2011.02.020.

1219 Schon, S. C., Head, J. W., 2012. Gasa impact crater, Mars: Very young gullies formed  
1220 from impact into latitude-dependent mantle and debris-covered glacier deposits?  
1221 Icarus, 218, 459-477, doi:10.1016/j.icarus.2012.01.002.

1222 Schon, S.C., Head, J.W., Fassett, C.I., 2009. Unique chronostratigraphic marker in  
1223 depositional fan stratigraphy on Mars: Evidence for ca. 1.25 Ma gully activity and  
1224 surficial meltwater origin. *Geology*, 37, 207-210, doi:10.1130/G25398A.1.

1225 Schorghofer, N., Edgett, K.S., 2006. Seasonal surface frost at low latitudes on Mars.  
1226 Icarus, 180, 321-334, doi:10.1016/j.icarus.2005.08.022.

1227 Schorghofer, N., Forget, F., 2012. History and anatomy of subsurface ice on Mars. *Icarus*,  
1228 220, 1112-1120, doi:10.1016/j.icarus.2012.07.003.

1229 Shinbrot, T., Duong, N.-H., Kwan, L., Alvarez, M.M., 2004. Dry granular flows can  
1230 generate surface features resembling those seen in Martian gullies. *Proc. Nat. Acad.*  
1231 *Sci.*, 101, 8542-8546, doi:10.1073/pnas.0308251101.

1232 Sylvest, M. S., Conway, S. J., Patel, M. R., Dixon, J. C., Barnes, A., 2016. Mass wasting  
1233 triggered by seasonal CO<sub>2</sub> sublimation under Martian atmospheric conditions:  
1234 Laboratory experiments. *Geophys. Res. Lett.*, 43, 12,363-12,370,  
1235 doi:10.1002/2016GL071022.

1236 Thomas, N., Hansen, C. J., Portyankina, G., Russell, P. S., 2010. HiRISE observations of  
1237 gas sublimation-driven activity in Mars' southern polar regions: II. Surficial deposits  
1238 and their origins. *Icarus*, 205, 296-310, doi:10.1016/j.icarus.2009.05.030.

1239 Treiman, A.H., 2003. Geologic settings of Martian gullies: Implications for their origins.  
1240 *J. Geophys. Res.*, 108, 8031-8042, doi:10.1029/2002JE001900.

1241 Turnbull, B., Bowman, E. T., McElwaine, J. N., 2015. Debris flows: Experiments and  
1242 modelling. *Comp. Rend. Phys.*, 16, 86-96.

1243 Vincendon, M., 2015. Identification of Mars gully activity types associated with ice  
1244 composition. *J. Geophys. Res. Planets*, 120, doi:10.1002/2015JE004909.

1245 Vincendon, M., Forget, F., Mustard, J., 2010a. Water ice at low to midlatitudes on Mars.  
1246 *J. Geophys. Res.*, 115, E10001, doi:10.1029/2010JE003584.

1247 Vincendon, M., Mustard, J., Forget, F., Kreslavsky, M., Spiga, A., Murchie, S., Bibring,  
1248 J.-P., 2010b. Near-tropical subsurface ice on Mars. *Geophys. Res. Lett.*, 37, L01202,  
1249 doi:10.1029/2009GL041426.

1250 Williams, K. E., Toon, O. B., Heldmann, J. L., Mellon, M. T., 2009. Ancient melting of  
1251 mid-latitude snowpacks on Mars as a water source for gullies. *Icarus*, 200, 418-425,  
1252 doi:10.1026/j.icarus.2008.12.013.

1253 Wordsworth, R. D., 2016. The climate of early Mars. *Annu. Rev. Earth Planet. Sci.*, 44,  
1254 381-408, doi:10.1146/annurev-earth-060115-012355.

1255 Zurek, R.W., Smrekar, S.E., 2007. An overview of the Mars Reconnaissance Orbiter  
1256 (MRO) science mission. *J. Geophys. Res.*, 112, E05S01, doi:10.1029/2006JE002701.  
1257  
1258



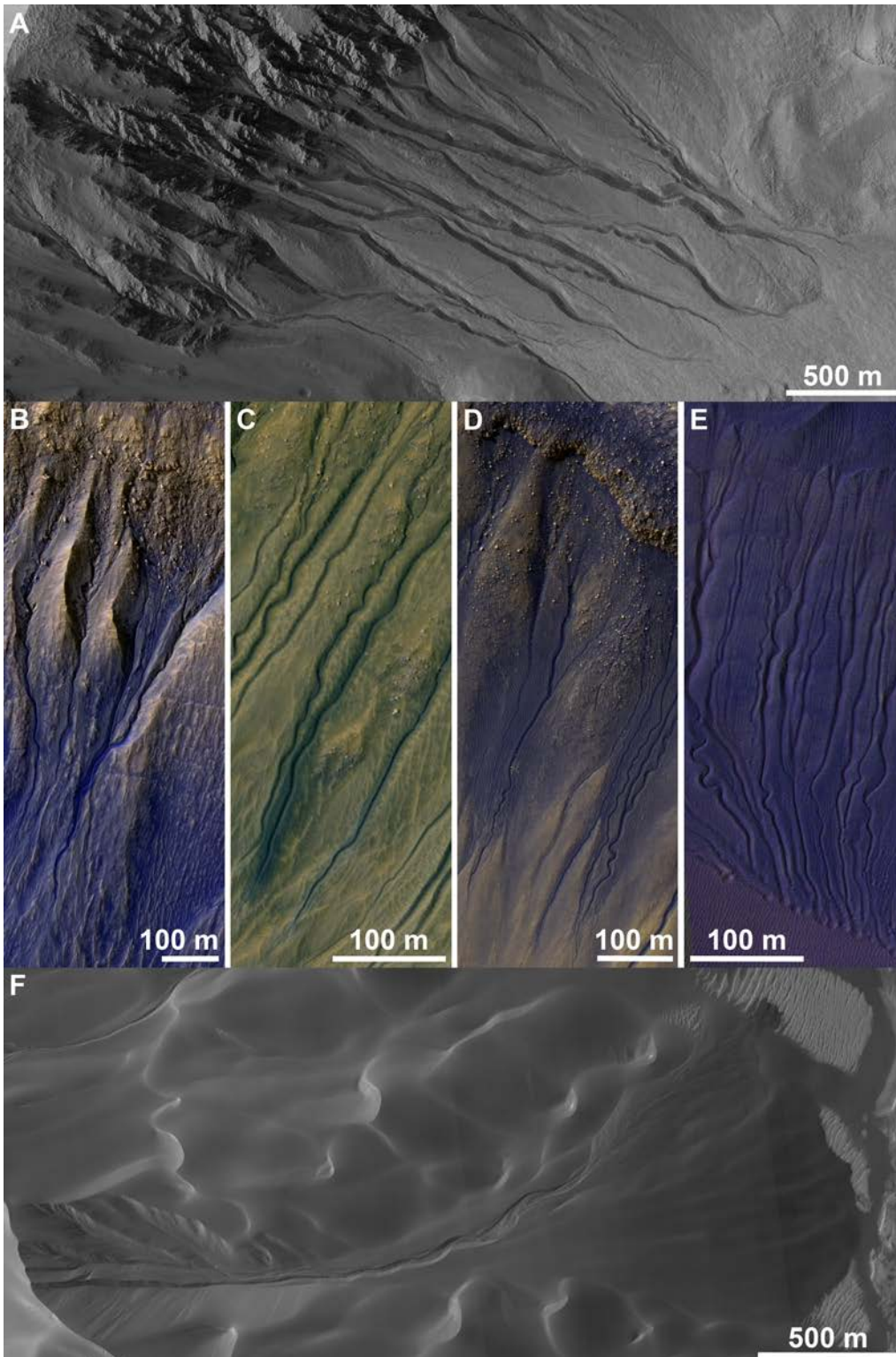
1260 **Table 1. Comparison of Gully Observations and Dry Frost Model**

Observation	Frost Model Interpretation
Widespread gully activity, consistent with all fresh gullies being active on timescales of centuries.	Key observation supporting frost model.
Current activity associated with seasonal frost, primarily CO <sub>2</sub> .	Key observation supporting frost model.
Diverse aqueous-like (fluvial or debris flow-like) morphologies in gullies.	Observed to form by current processes (see main text for further discussion).
Gullies concentrated in mid-latitudes, occasionally high latitude, and are relatively uncommon in Hellas basin and northern plains.*	Distribution represents overlap of frost abundance (minimal near equator) and topographic roughness/steep slopes (rare at high latitude and on plains).
Mid-latitude gullies face the pole.*	Consistent with observed frost distribution.
High-latitude gullies face equator or have no preference.*	Consistent with observed frost distribution.
Equatorial gullies exist, but are less developed (McEwen et al., 2016).	Due to minor frost and/or RSL; should show minimal fluidization beyond typical dry mass movements.
Gullies initiate on steep slopes.*	Steep slopes are less stable, more easily eroded; may also be required to permit frost accumulation at lower latitudes.
Gullies found at a wide range of elevations.*	CO <sub>2</sub> frost found at all elevations; frost point varies < 10 K over typical gully elevations.
Gullies found on sand dunes and isolated peaks.*	Consistent with frost deposited from atmosphere.
Gullies associated with low dust cover, low albedo, intermediate grain size at coarse scales (Harrison et al., 2015).	May be proxy for other favorable conditions; thermophysical classes correlate with latitude.
Gullies are not routinely associated with hydrated minerals (Núñez et al., 2016).	Consistent with no frequent or long-lived water-rock interactions.
Apparent reduction in gully fluidization in recent events (Kolb et al., 2010b).	Frost process intensity varies over time; alternatively, may represent local effects at the small number of sites.
Episodic formation by many events, with channel abandonment (Dickson and Head, 2009).	Current activity is the most recent generation of ongoing formative events. Channel abandonment observed.
Age $\leq$ ~1 Ma (e.g., Reiss et al., 2004; Schon et al., 2009; Raack et al., 2012).	Consistent with ongoing formation. Most gullies are un-cratered.
Northern hemisphere gullies appear more degraded/eroded than those in the south (Heldmann et al., 2007).	Lower current activity rate in northern gullies, due to occurrence of perihelion in northern fall.
Buried and/or inactive gullies exist (e.g.,	Due to variations in the distribution of

Morgan et al., 2010; Raack et al., 2012; Dickson et al., 2015a).	seasonal frost processes over time (cf. Pilorget and Forget, 2016).
Gullies commonly incised into mid-latitude mantle (e.g., Christensen, 2003).	Mantle readily eroded by frost processes when not ice-cemented. Bedrock is more resistant to erosion and mobilization.
Occasional association with bedrock layers (e.g., Malin and Edgett, 2000; Gilmore and Phillips, 2002).	Consistent with erosion of material up to resistant layers.
Gully fan outcrops expose boulders (de Haas et al., 2015c).	Current processes observed to transport and bury boulders within channels and on fans.
Small lunar mass-wasting features resemble poorly developed gullies with straight channels (Bart, 2007; Kumar et al., 2013).	Demonstrates that simple forms can develop with no volatile; larger, well-developed features require frost processes.

1261 \*Major surveys of the distribution and properties of gullies include Malin and Edgett  
1262 (2000), Heldmann and Mellon (2004), Heldmann et al. (2007), Balme et al. (2006),  
1263 Bridges and Lackner (2006), Dickson et al. (2007), Dickson and Head (2009), Kneissl et  
1264 al. (2010), and Harrison et al. (2015).  
1265  
1266

1267 **Figure Captions**

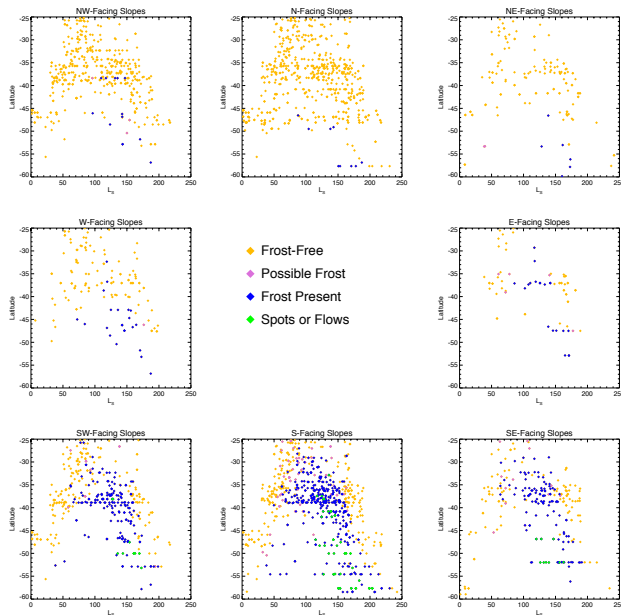


1268

1269 **Figure 1.** Examples of gully morphologies. A) Examples of classic alcove-channel-apron

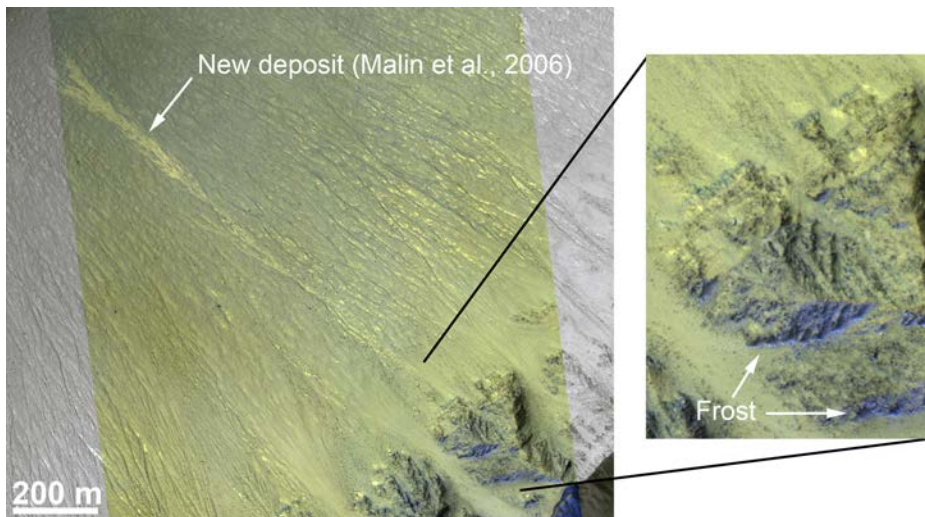
1270 gullies cut into the wall of Triolet crater (37.1°S, 191.9°E). B–E show a gradation from

1271 classic crater-wall gullies towards linear dune gullies. B) Alcove-channel-apron gullies  
 1272 cut into mid-latitude mantle material, but with minor sand coloration/infill. C) Gullies  
 1273 with distinct channels but minor alcoves and depositional aprons, cut into a substrate with  
 1274 some large ripples but without the coloration of sand. D) Gullies in crater-wall material  
 1275 that appears to be a mix of sand and other material. E) Linear dune gullies (channels with  
 1276 minimal alcoves or deposits, and common terminal pits) in sand, including sinuous  
 1277 examples. F) Large dune gully in Matara crater (49.5°S, 34.9°E) with classic alcove-  
 1278 channel-apron morphology. (A: HiRISE image PSP\_003583\_1425. B:  
 1279 ESP\_046309\_1425. C: ESP\_040402\_1410. D: ESP\_024344\_1325. E:  
 1280 ESP\_029701\_1295. F: ESP\_038387\_1300. Downhill is to the right in A and F and to the  
 1281 bottom in B–E. All image figures herein are sub-frames of HiRISE images (credit:  
 1282 NASA/JPL/University of Arizona) with north up and light from the left, and have been  
 1283 stretched to maximize local contrast. All original data are available via the Planetary Data  
 1284 System.)



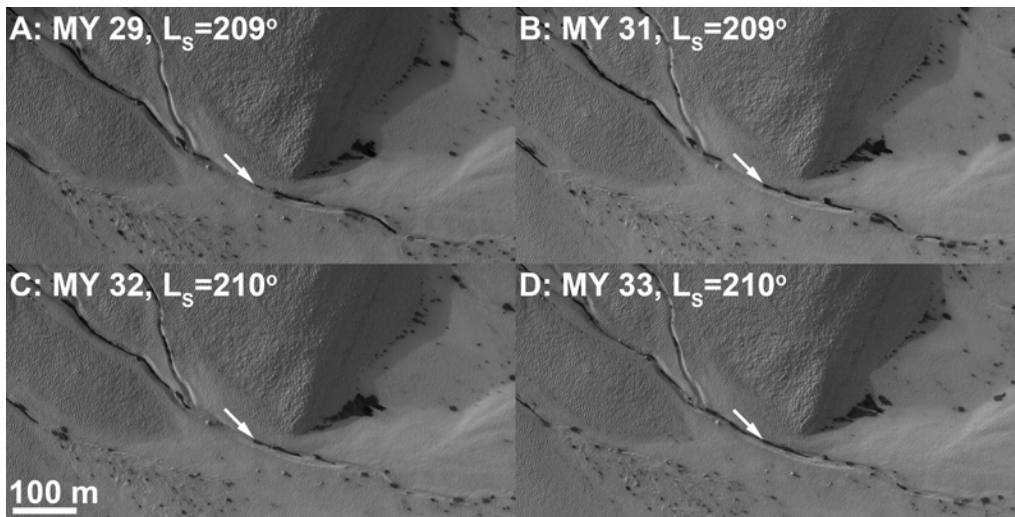
1285

1286 **Figure 2.** Seasonal frost (outside gully alcoves) in the southern hemisphere, as a function  
1287 of season and slope orientation.



1288

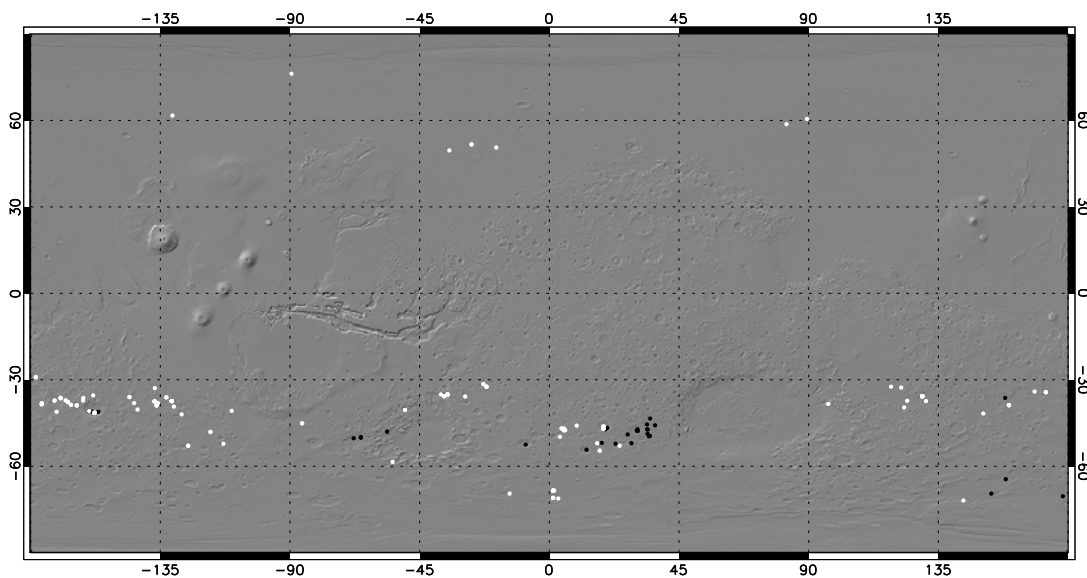
1289 **Figure 3.** One of the few equator-facing mid-latitude gully flows correlates with an  
1290 unusual small patch of frost. Local frost (blue-tinted material) occurred in hollows on a  
1291 broadly equator-facing slope uphill (lower right) from a new gully deposit in Penticton  
1292 crater (38.4°S, 96.8°E) at  $L_S=132^\circ$ . (HiRISE image ESP\_036578\_1415.)



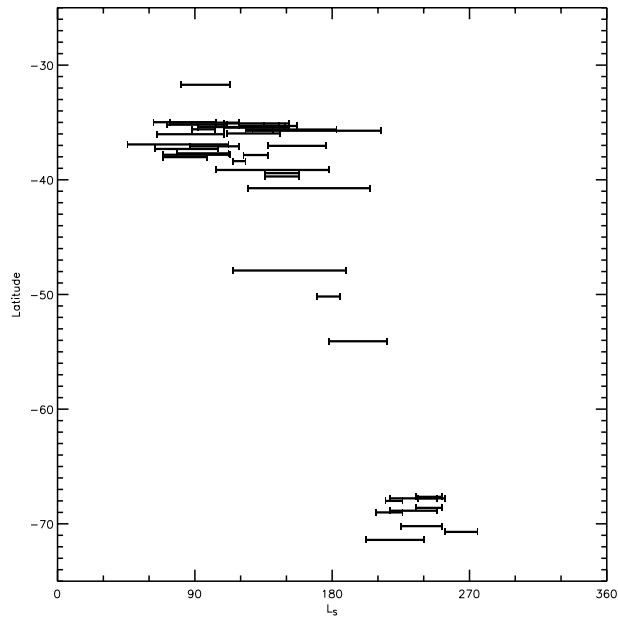
1293

1294 **Figure 4.** Example of defrosting flows in a polar pit gully (68.5°S, 1.3°E). Flows  
1295 concentrate in channels, gradually advance, and approximately repeat from year to year.  
1296 The flows are dark in contrast with the widespread frost and leave no resolvable sign in

1297 albedo or topography once the frost is gone. Arrows indicate the source point of a flow  
1298 for comparison between years. In (D), the flow is being overtaken by another flow  
1299 initiating higher in the channel. (A: HiRISE image ESP\_011963\_1115. B:  
1300 ESP\_029580\_1115. C: ESP\_038428\_1115. D: ESP\_047250\_1115. Downhill is to the  
1301 lower right.)



1302  
1303 **Figure 5.** Map of observed active gullies (white symbols) and active dune or sandy-slope  
1304 gullies (black). North polar dune alcoves (Hansen et al. 2015) and similar minor alcoves  
1305 on other dunes are not included here.



1306

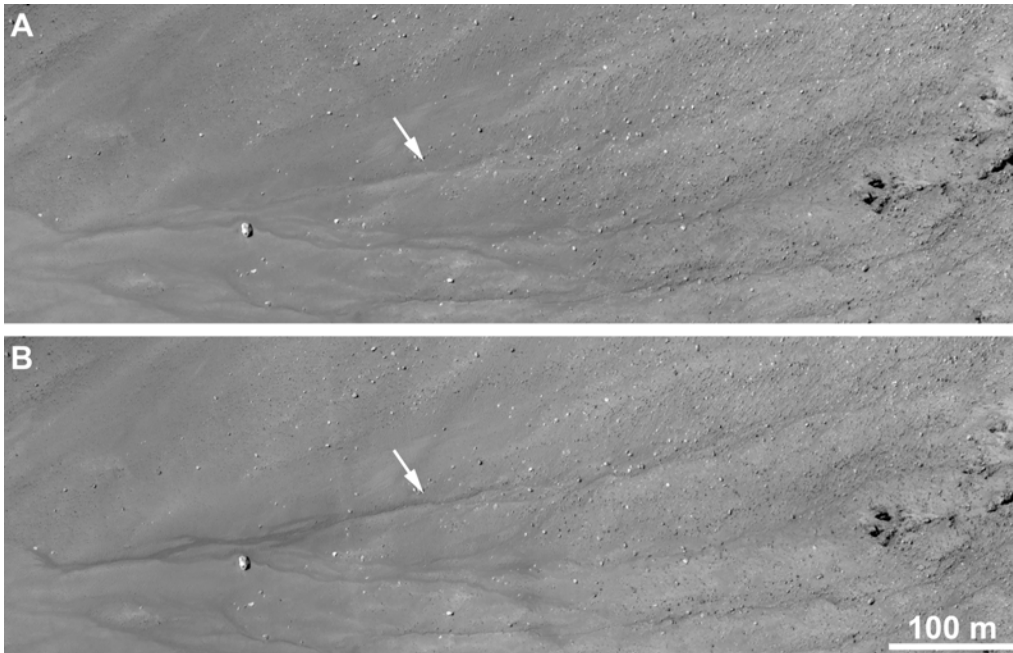
1307 **Figure 6.** Timing of well-constrained gully changes in the southern hemisphere as a  
 1308 function of latitude. Only changes constrained to an interval  $<90^\circ$  of  $L_S$  are shown. (Note  
 1309 that this is not quite a constant unit of time due to Mars' elliptical orbit.) Lines are offset  
 1310 in latitude by small amounts in order to separate overlapping intervals.



1311

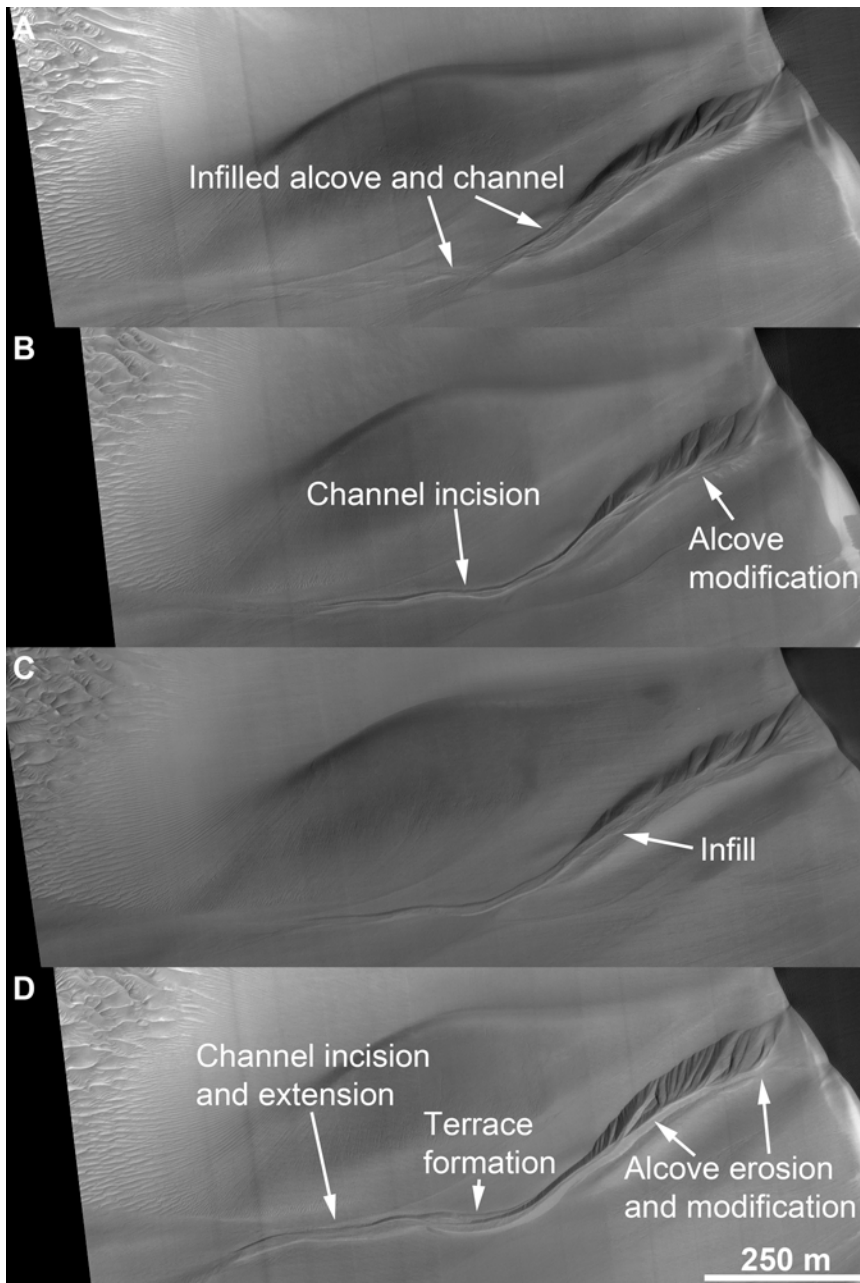
1312 **Figure 7.** Gully flows in Selevac crater (37.4°S, 228.9°E). The flows bury or disrupt  
1313 seasonal frost, allowing the shape of the entire mass movement to be seen. They begin at  
1314 point sources (arrows), descend along channels, and terminate in extensive deposits. The  
1315 image is in shadow and has been stretched to show detail, saturating the illuminated  
1316 areas; original data available via the Planetary Data System. (HiRISE image  
1317 ESP\_045158\_1425.)





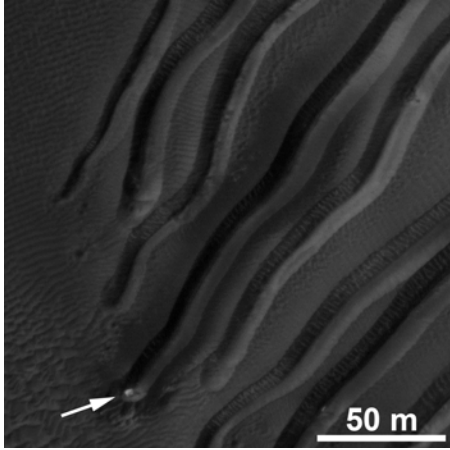
1318

1319 **Figure 8.** Activity in Raga crater (48.1°S, 242.4°E) showing gully formation. An ill-  
1320 defined shallow trough or degraded gully seen in MY 29 (A) subsequently became active.  
1321 Two flow events occurred, resulting in a much more sharply-defined channel system (B).  
1322 (A: HiRISE image ESP\_014011\_1315. B: ESP\_040239\_1315. Downhill is to the left.)



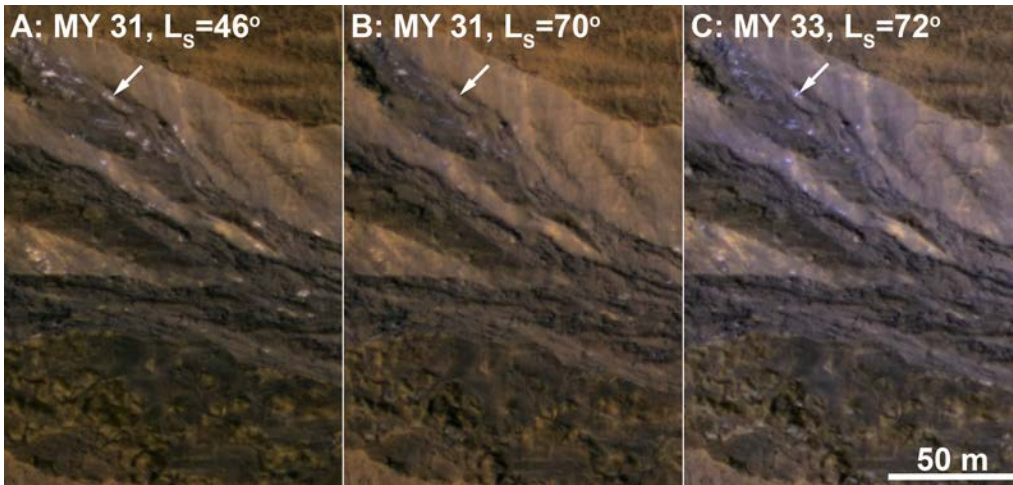
1323

1324 **Figure 9.** Major changes in a dune gully west of the Argyre basin (48°S, 303.7°E),  
 1325 progressing from a degraded alcove and obliterated apron (A) to a sharply defined system  
 1326 with a large, terraced channel (D). Panels B–C show incremental annual changes, which  
 1327 can each be dated to Martian winter. (A: HiRISE image ESP\_023582\_1315. B:  
 1328 ESP\_030584\_1315. C: ESP\_038087\_1315. D: ESP\_047331\_1315. Downhill is to the  
 1329 left.)



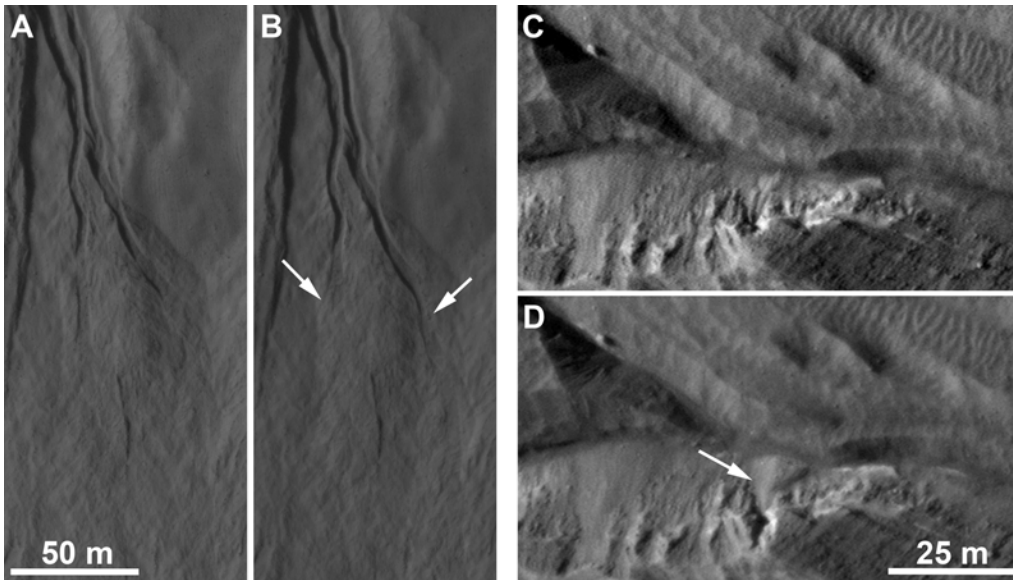
1330

1331 **Figure 10.** Ice slab and dark halo at the toe of a large linear dune gully in Russell crater  
 1332 (54.3°S, 12.9°E). The halo is interpreted to form via sand thrown out by the sliding ice  
 1333 block, maintaining and incising the channel (Diniega et al., 2013). (HiRISE image  
 1334 ESP\_047078\_1255. Downhill is to the lower left.)



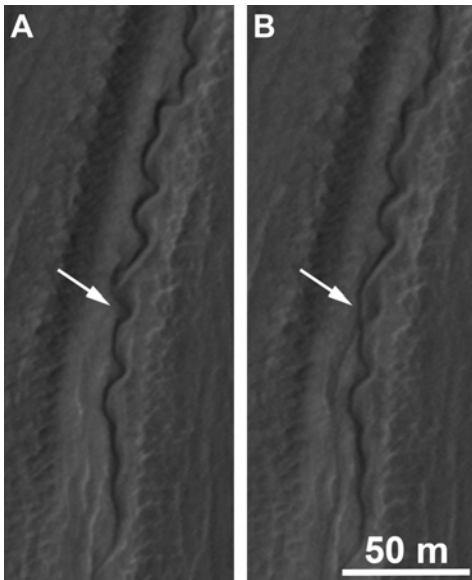
1335

1336 **Figure 11.** Likely ice exposure in mid-latitude mantle materials in a gully alcove  
 1337 (59.5°N, 302.2°E). Bright spots appeared prominent in mid-spring of MY 31 but faded  
 1338 over several months. They were again prominent, but with a different pattern, in MY 33.  
 1339 Arrow indicates an example of one of the spots. (A: HiRISE image ESP\_025322\_2400.  
 1340 B: ESP\_026021\_2400. C: ESP\_043691\_2400. Downhill is to the right.)



1341

1342 **Figure 12.** Examples of channel changes in gullies. A–B) A flow event in this gully in  
 1343 eastern Hale crater (35.1°S, 324.7°E) divided between two channels. The arrows indicate  
 1344 that in one (left), deposition obliterated part of the channel system, while in the other  
 1345 (right), the channel was extended. Distributed changes due to deposition occur  
 1346 throughout the bottom of the frames. C–D) A flow in Triolet crater (37.1°S, 191.9°E)  
 1347 disturbed material along the edge of the channel, causing a small hollow to collapse and  
 1348 form a small debris cone within the channel. (A: HiRISE image ESP\_011819\_1445. B:  
 1349 ESP\_038218\_1445. C: ESP\_020751\_1425. D: ESP\_047190\_1425. Downhill is to the  
 1350 bottom in A–B and to the right in C–D.)

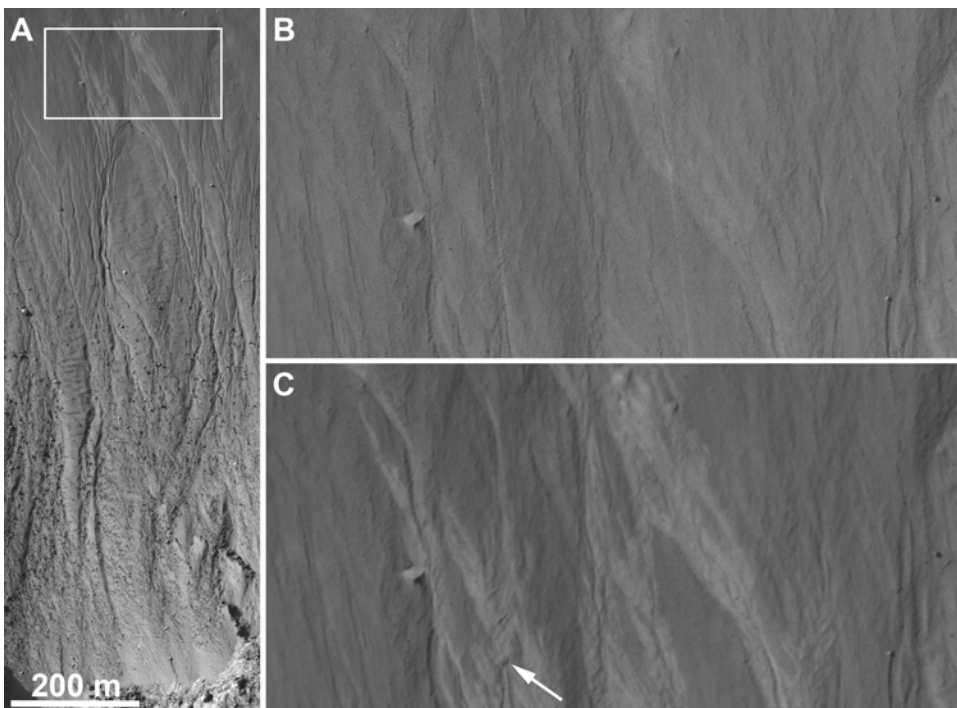


1351

1352 **Figure 13.** Cutoff of a sinuous curve (arrow) by a new incised segment in a gully channel

1353 within sandy fill in a crater-wall gully (38.9°S, 196°E). (A: HiRISE image

1354 ESP\_029032\_1410. B: ESP\_046702\_1410. Downhill is to the bottom.)

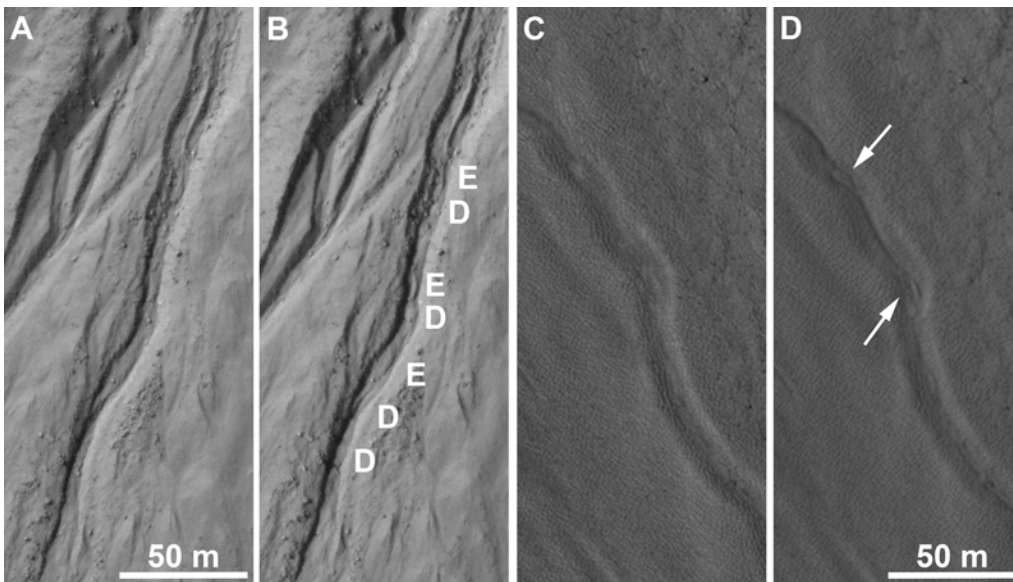


1355

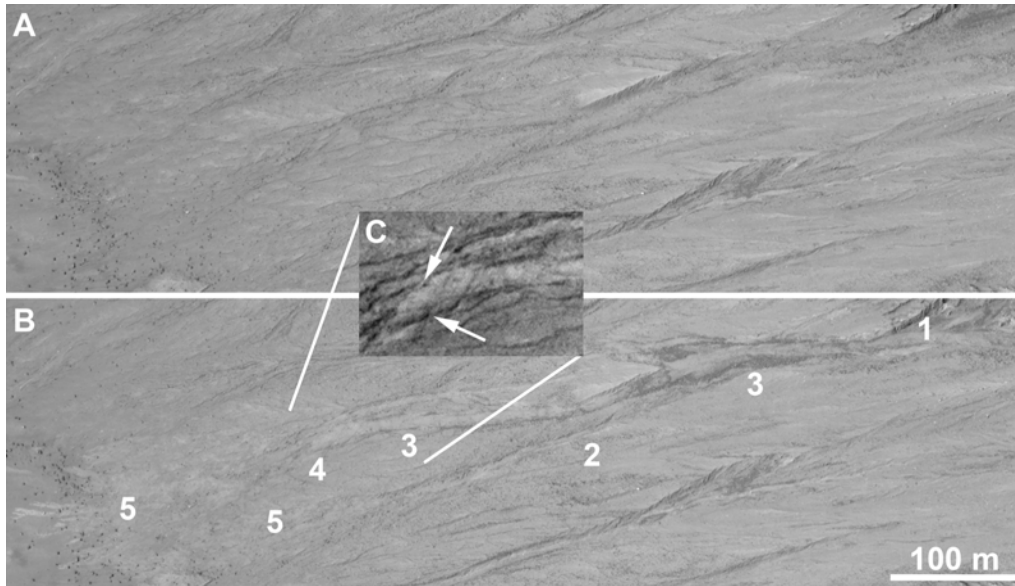
1356 **Figure 14.** Example of branching flow producing activity in multiple channels, located in

1357 Asimov crater (46.8°S, 4.3°E). A) Overview of gully system, with complex channel

1358 network. Box indicates location of panels B–C. B) “Before” image showing faint light  
1359 material associated with some channels. C) “After” image with distinct bright deposits  
1360 branching and occupying different channels, breaking out in some cases. Deposition  
1361 producing a topographic change (arrow) demonstrates that this is real activity and not a  
1362 photometric effect. (A, C: HiRISE image ESP\_036977\_1330. B: PSP\_002179\_1330.  
1363 Downhill is to the top.)



1364  
1365 **Figure 15.** Examples of changes in channels. A–B) Alternating erosion and deposition  
1366 (“E” and “D” annotations) produced by local conditions, resulting in small-scale bar-like  
1367 landforms within the channel (38.1°S, 224°E). C–D) Incision within an older, larger  
1368 channel (47.5°S, 5.5°E), resulting in formation or enhancement of an “island” (upper  
1369 arrow) and a lobate bar-like feature (lower arrow). (A: HiRISE image  
1370 ESP\_023809\_1415. B: ESP\_047057\_1415. C: ESP\_013334\_1320. D:  
1371 ESP\_047276\_1320. Downhill is to the bottom in all panels.)



1372

1373 **Figure 16.** Changes within a gully system in Istok crater (45.1°S, 274.2°E), which either  
 1374 divided between two gullies or encompassed multiple events closely spaced in time.

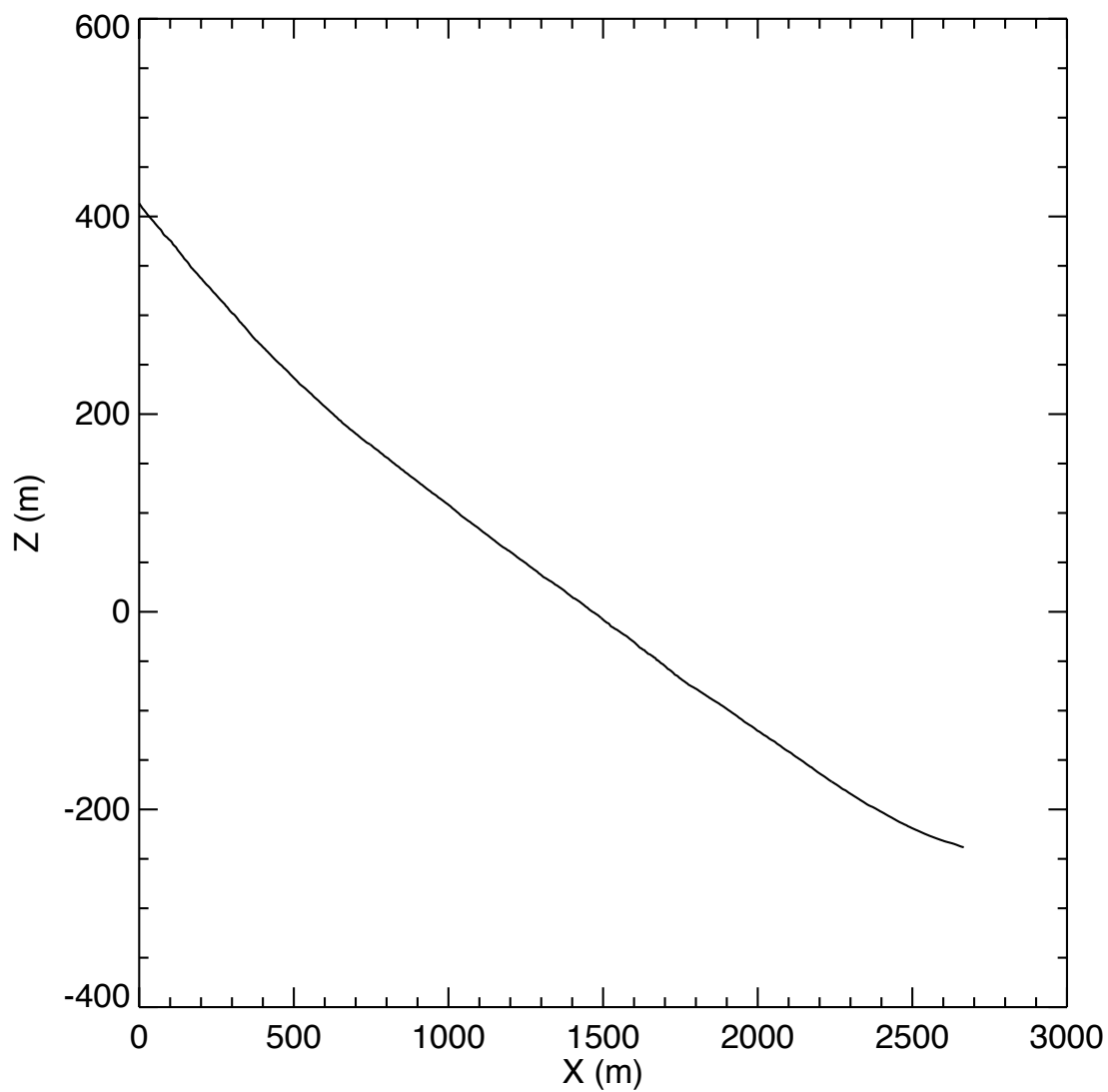
1375 Numbers indicate source alcove (1), local scour of a channel segment (2), deposition of  
 1376 dark boulder-rich levees (3), formation of a lobate deposit snout (4), and distributed  
 1377 topographic changes (sufficient to move and/or bury rocks) (5). Note that the most distal

1378 deposits are small, relatively-bright toes, although the deposit mostly matches the tone of  
 1379 the upper slope and thus lacks contrast. Inset C) shows an enlarged view of the lobate

1380 snout (4) from a low-Sun image to emphasize topography with arrows indicating

1381 margins. (A: HiRISE image ESP\_040251\_1345. B: ESP\_048255\_1345. C:

1382 ESP\_045842\_1345. Downhill is to the left.)



1383

1384 **Figure 17.** Longitudinal profile of the large alcove-channel-apron dune gully in Matara

1385 crater (Fig. 1f) derived from a HiRISE Digital Terrain Model

1386 (DTEEC\_022115\_1300\_22392\_1300\_U01). Using definitions from Conway et al.

1387 (2015), this profile has concavity measures  $A_{ero}=0.14$  (Mars gully range 0.02–0.77 from

1388 Conway et al. (2015),  $E_q=0.28$  (Mars range 0.11–0.63),  $CI=0.07$  (Mars range -0.16–0.3),

1389 and  $\theta=-0.23$  (Mars range -0.86–0.02). The slope is over  $20^\circ$  near the head of the gully



1390 (and may be higher on alcove slopes above the thalweg) and below  $10^\circ$  near the flow

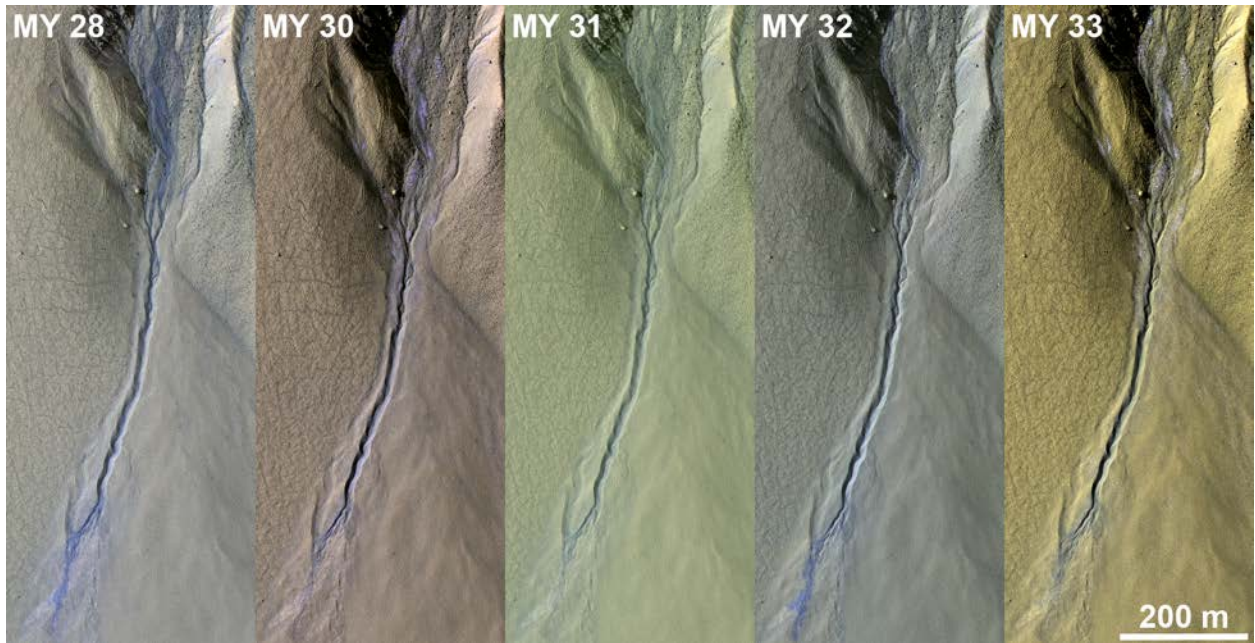
1391 termination.

1392

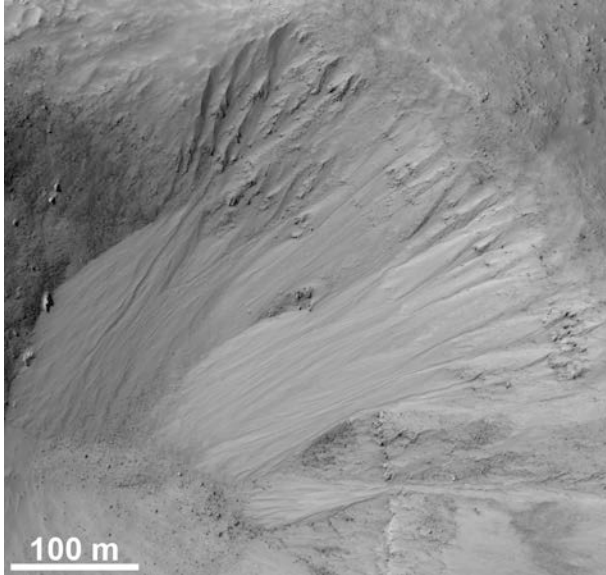
## Supplementary Materials for “The Formation of Gullies on Mars Today”

The supplementary information for this report includes figures, animations, and a summary table describing details of known gully activity. Original HiRISE images are available via the Planetary Data System, including both raw spacecraft data and the Reduced Data Records used for these figures. Some images have been stretched to improve contrast.

### Supplementary Figures

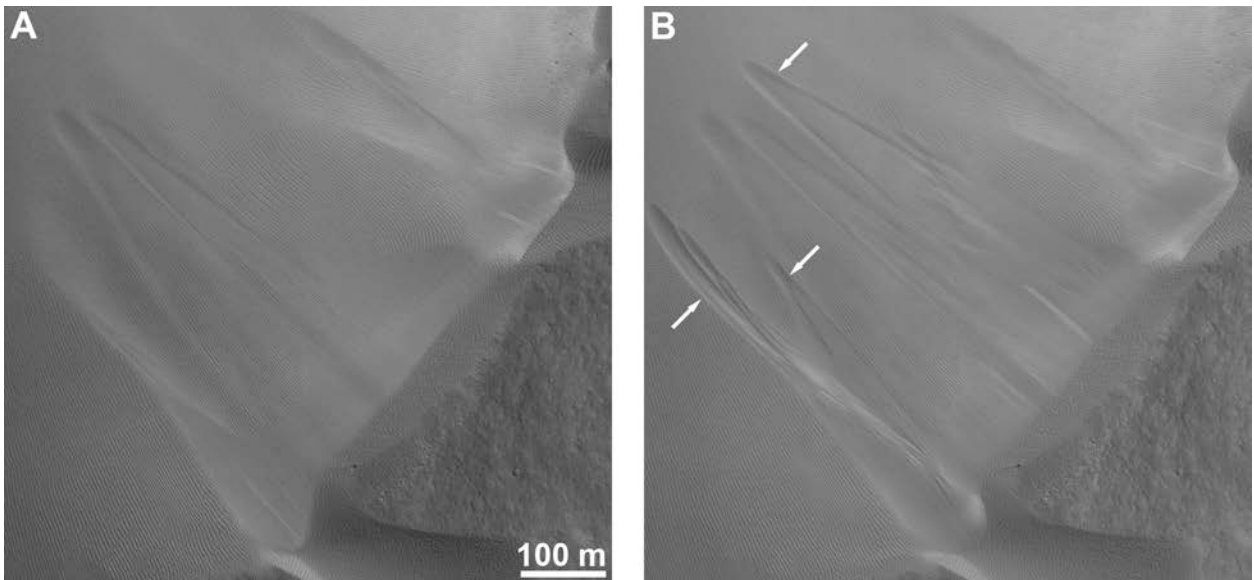


**Supplementary Figure 1.** Rapid changes in the appearance of deposits associated with a gully at 54.5°S. The deposit appeared fresh in MY 28, but was largely faded in MY 30–31. In MY 32, a new dark deposit formed, with accompanying morphologic changes including minor channel incision. This deposit had mostly faded by MY 33. This demonstrates that distinct deposits can fade on short timescales, and also that frequent activity can occur in individual gullies. (HiRISE color images PSP\_003695\_1250, ESP\_020863\_1250, ESP\_030344\_1250, ESP\_038546\_1250, and ESP\_047302\_1250. Images have relative stretch to maximize contrast despite variable frost, illumination, and atmospheric dust, so absolute color is not directly comparable across images.)



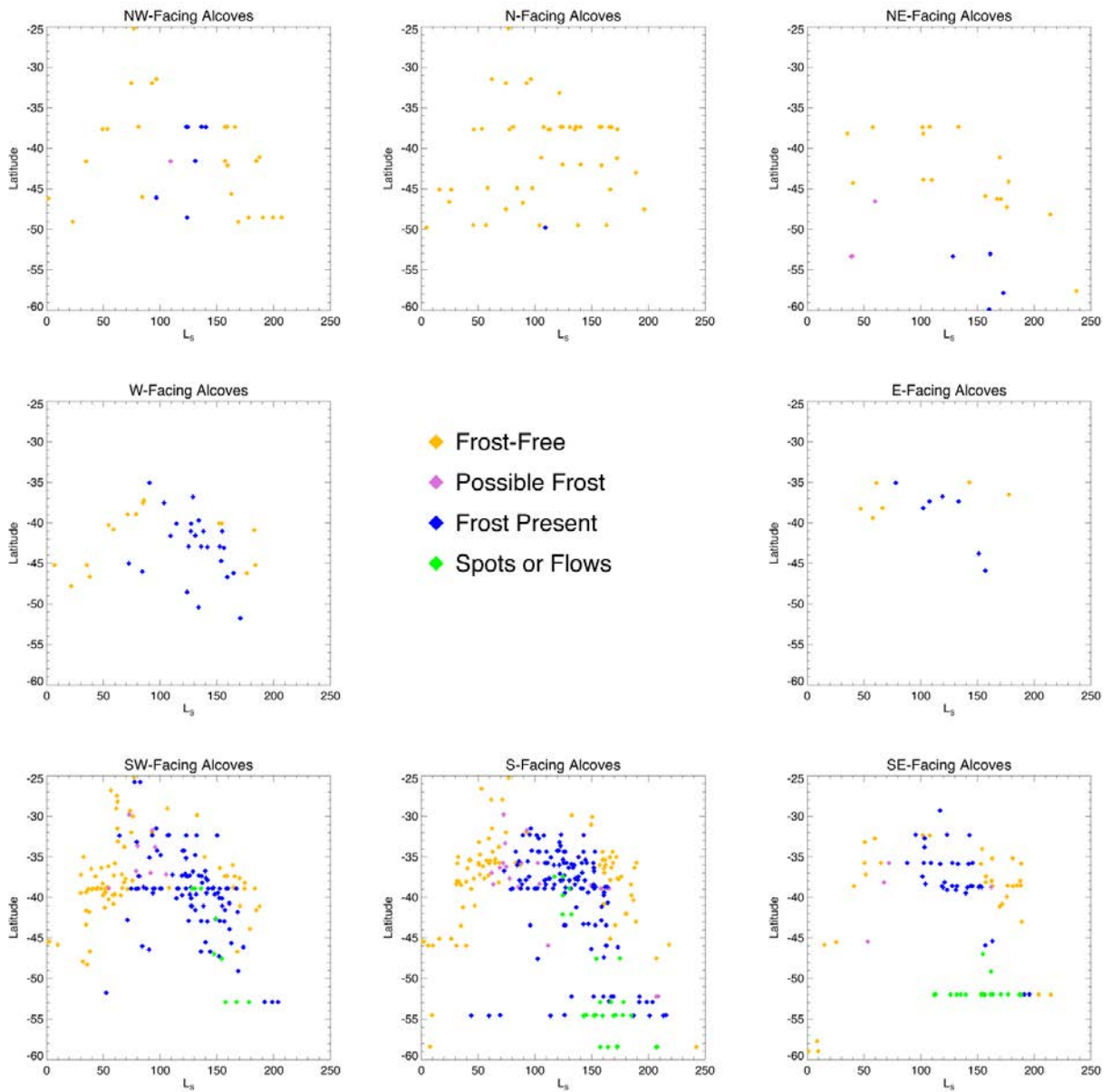
1415  
1416  
1417  
1418  
1419  
1420  
1421  
1422  
1423  
1424

**Supplementary Figure 2.** Equatorial gully-like landforms (McEwen et al., 2016) in an unnamed crater at 2.6°N latitude. Water frost is observed at low latitudes in the southern hemisphere (Vincendon et al., 2010a) and perhaps traces are enough to occasionally trigger mass movements and gully formation. Nighttime CO<sub>2</sub> frost also occurs in low-thermal inertia regions at the equator (Piqueux et al., 2016), and H<sub>2</sub>O frost has been observed on the *Opportunity* rover in the early morning (Landis et al., 2007). However, equatorial gullies have not been studied in sufficient detail to understand how they relate to the more prominent mid-latitude features. (HiRISE image ESP\_034864\_1825.)



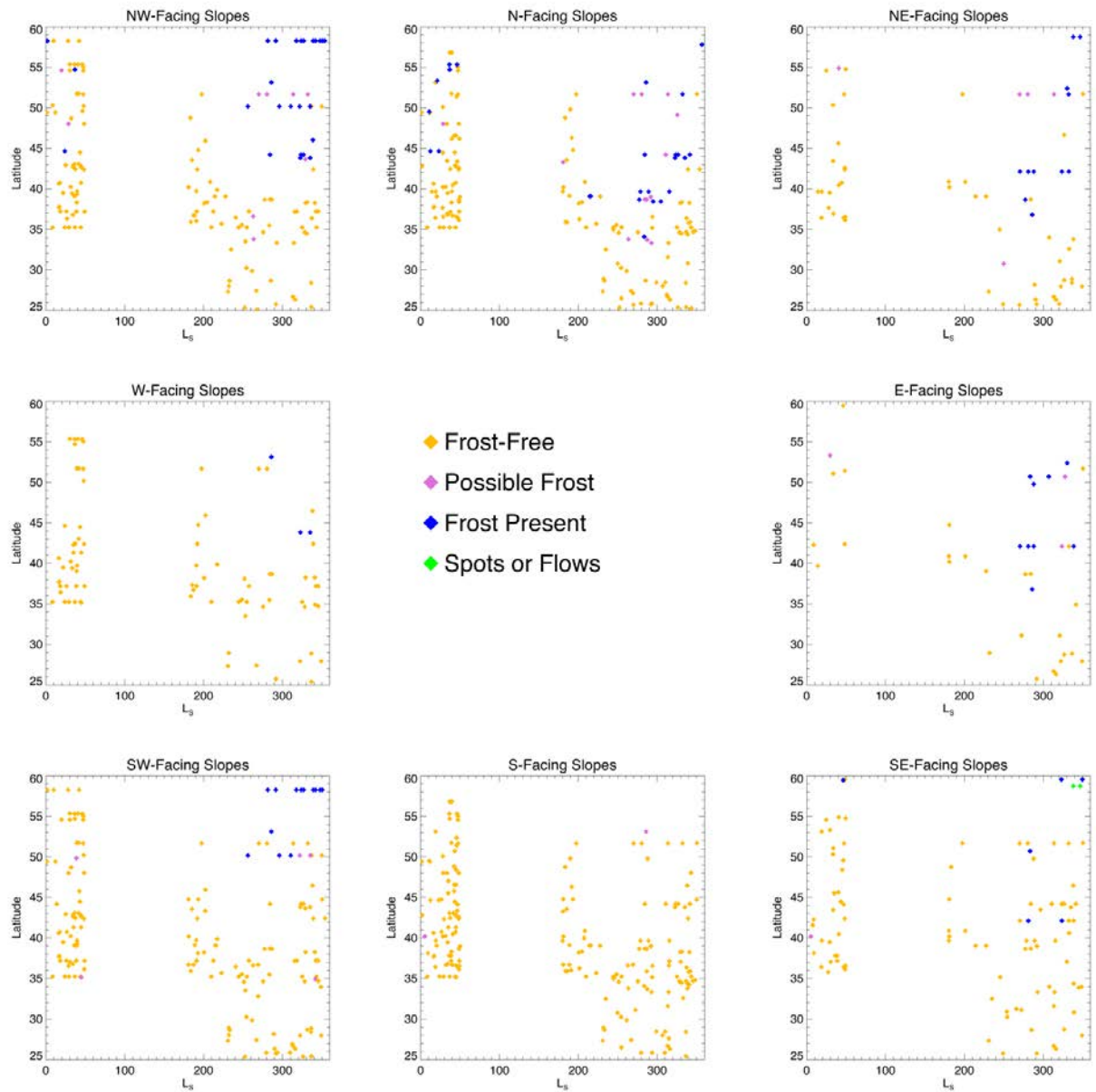
1425  
1426  
1427  
1428  
1429  
1430

**Supplementary Figure 3.** Large-scale, leaved, lobate flows formed in sand covering an equatorial crater wall in Meroe Patera (7.2°N, 67.8°E), demonstrating that these morphologies can form with little or no volatiles (HiRISE images ESP\_039388\_1875 and ESP\_040588\_1875.)



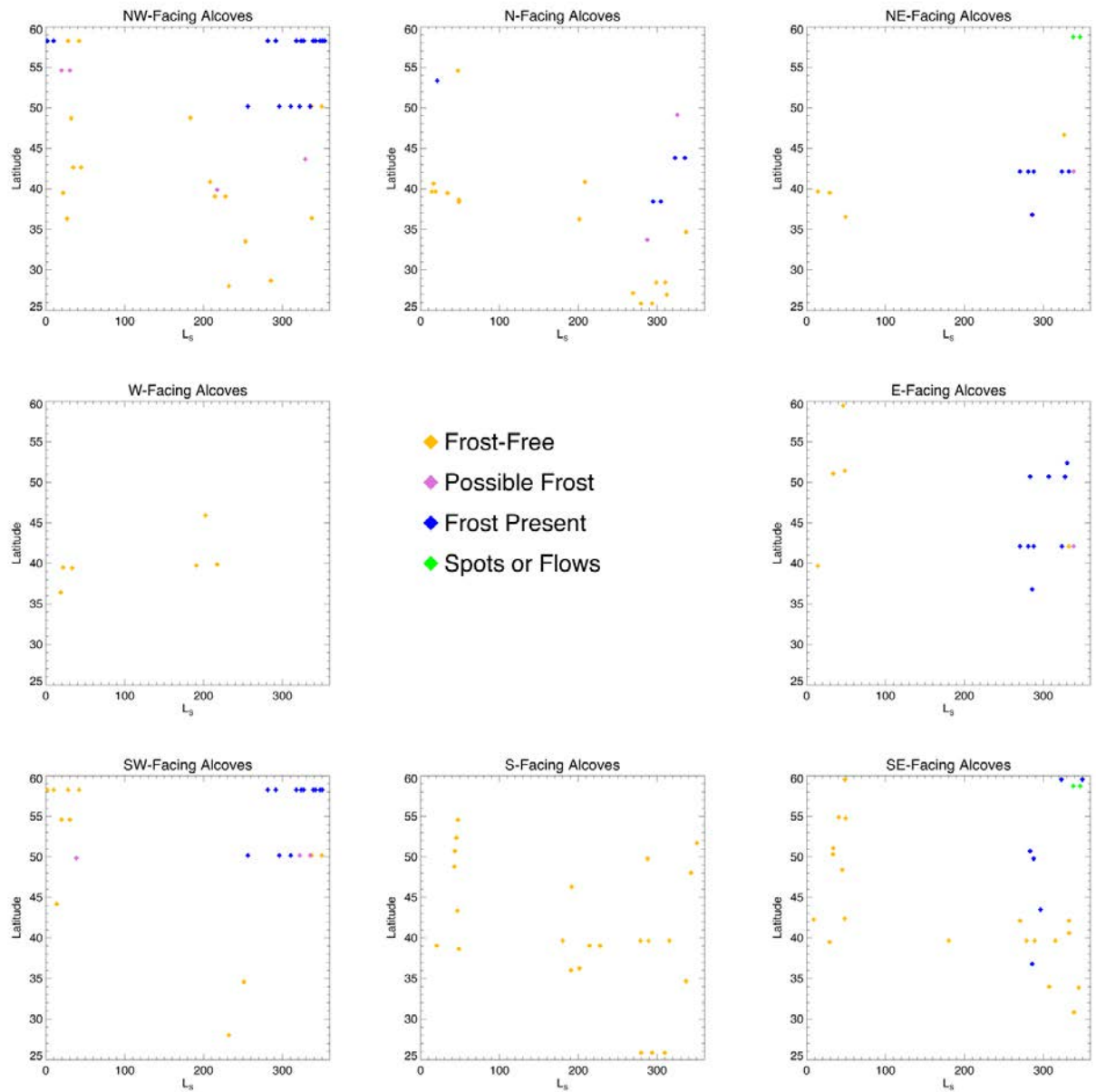
1431  
 1432  
 1433  
 1434  
 1435

**Supplementary Figure 4.** Observations of frost within moderately to well-developed gully alcoves in the southern hemisphere (compare with main text Fig. 2, which shows non-gullied slopes and poorly developed, shallow alcoves).



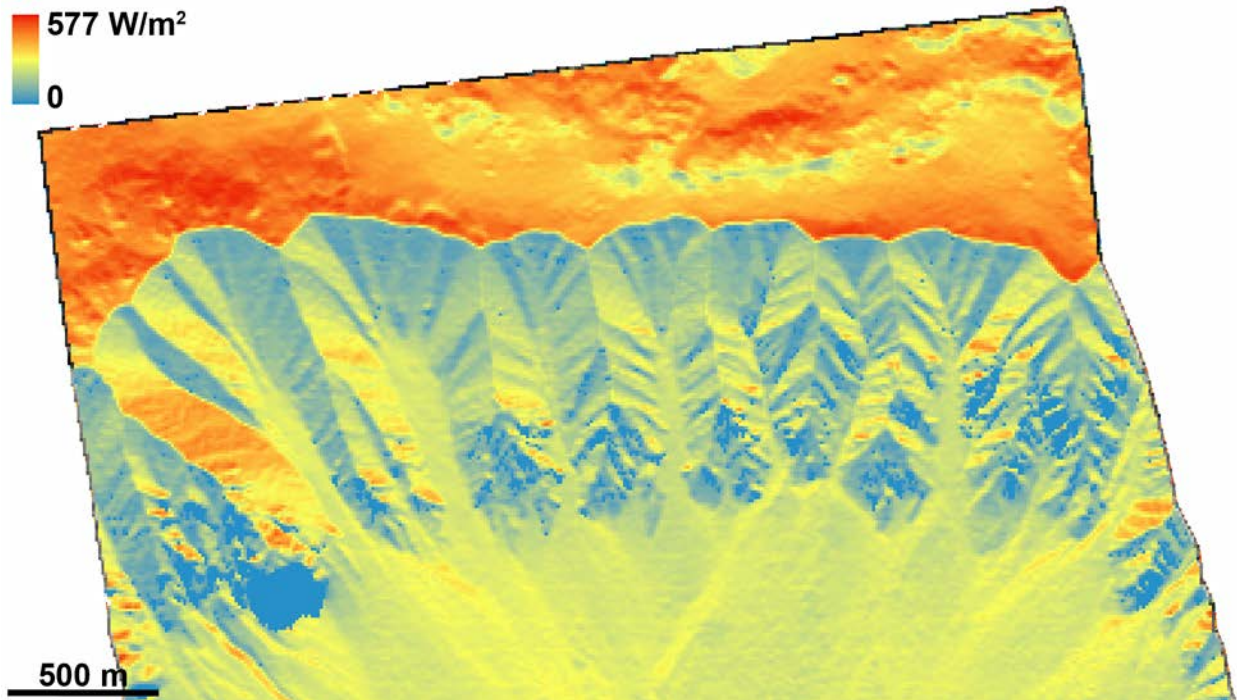
1436  
 1437  
 1438  
 1439

**Supplementary Figure 5.** Observations of frost on non-gully slopes or in poorly developed alcoves in the northern hemisphere.



1440  
 1441  
 1442

**Supplementary Figure 6.** Observations of frost within moderately to well-developed gully alcoves in the northern hemisphere.



1443  
1444  
1445  
1446  
1447  
1448  
1449  
1450  
1451  
1452  
1453  
1454

**Supplementary Figure 7:** Modeled insolation in Gasa crater at noon at  $L_S=150^\circ$  (late winter, after most activity has concluded), assuming a clear atmosphere. Insolation was modeled based on the slopes and aspects of a DTM resampled to 10 m/pix. The insolation in even the best-illuminated parts of the gully alcoves is just over  $400 \text{ W/m}^2$ . This heat input is far below the heat loss for  $\text{H}_2\text{O}$  ice approaching the melting temperature, so frost or ice cannot melt at the times and places of gully activity. For pure water frost, latent heat loss to sublimation alone exceeds this insolation at temperatures below the melting point (Ingersoll, 1970; Hecht, 2002). Additionally, radiative heat loss at 273 K is  $315 \text{ W/m}^2$ , which could be reduced by a factor of  $\sim 2$  in these alcoves since roughly half of the sky is blocked by warmer ground, and conductive and convective heat losses also occur.

1455 **Supplementary Animations**

1456 The supplementary animations are time comparisons of selected changes which  
1457 highlight important morphological effects. Images used in the animations are selected for  
1458 similar illumination and viewing geometry, but are not orthorectified. (Orthorectified  
1459 images are not always available, and entail some loss of detail due to resampling.) There  
1460 is thus typically some distortion between the frames which appears as a stretch or twist of  
1461 the surface, but the comparisons have been selected to minimize distortion and maximize  
1462 visibility of the changes.

1463 The animations are provided as separate animated gif files. Descriptions of each  
1464 animation are below.

1465  
1466 **Supplementary Animation 1:** Gully initiation in Raga crater (48.1°S, 242.5°E);  
1467 compare with main text Fig. 8. Two separate events between the images resulted in  
1468 formation of a well-defined channel following a pre-existing crease in the topography,  
1469 possibly a degraded or infilled old channel. The images have near-identical illumination  
1470 (ESP\_014011\_1315: incidence angle 41.9°, phase angle 43.4°, subsolar azimuth 208.1°;  
1471 ESP\_040239\_1315: incidence angle 41.1°, phase angle 40.8°, subsolar azimuth 203.8°).  
1472

1473 **Supplementary Animation 2:** Gully changes in Dunkassa crater (37.5°S, 222.9°E). Two  
1474 separate events between the images resulted in channel abandonment and breakout,  
1475 forming a new 50-meter channel and terminal deposit. Sinuous curves in the upper  
1476 channel migrated downhill (arrows indicate outermost point of the bends). The images  
1477 have near-identical illumination (ESP\_013115\_1420: incidence angle 41.2°, phase angle  
1478 47.1°, subsolar azimuth 183.6°; ESP\_039488\_1420: incidence angle 42.2°, phase angle  
1479 47.6°, subsolar azimuth 183.1°).  
1480

1481 **Supplementary Animation 3:** Channel changes in an unnamed crater (compare main  
1482 text Fig. 13). Note migration of curves by erosion of the outer, downhill part of the curve,  
1483 and cutoff of one meander by formation of a new channel reach. Substrate is likely sandy,  
1484 but gullies are largely cut into mantle material. The images have near-identical  
1485 illumination (ESP\_029032\_1410: incidence angle 63.8°, phase angle 61.3°, subsolar  
1486 azimuth 200.1°; ESP\_046702\_1410: incidence angle 61.2°, phase angle 58.6°, subsolar  
1487 azimuth 201.8°).  
1488  
1489  
1490



1491 **Supplementary Tables**

1492 Supplementary Table 1 summarizes information about known gully changes on  
 1493 Mars. As noted in the main text, some changes are likely missed because of poor image  
 1494 conditions or poor match in lighting and/or geometry; therefore, this is a lower bound on  
 1495 gully activity in existing data. Only definite changes are reported here; additional  
 1496 possible and probable changes have been observed but are considered unconfirmed for  
 1497 various reasons. Typically, this is because either the quality of the comparison data is  
 1498 poor (e.g., shadows over the gullies), the comparison images are a poor match (very  
 1499 different illumination or spacecraft geometry), or because the effects of the change are  
 1500 subtle. These factors can trade off against each other—subtle changes may be considered  
 1501 confirmed if there is an extremely good match in lighting and viewing angles. It is likely  
 1502 that these candidate changes will eventually be tested, and some confirmed, by  
 1503 acquisition of additional data. In some cases where multiple changes occurred, only the  
 1504 most prominent are enumerated, as it is not practical to give all the details of assorted  
 1505 minor changes.

1506 Most of the changes recorded here were first observed in this project or  
 1507 predecessor work (Dundas et al., 2010; 2012; 2015; Diniega et al., 2010). To our  
 1508 knowledge, the first definite observation of gully changes on Mars was in a Mars Orbiter  
 1509 Camera captioned image release by Malin and Edgett (2005;  
 1510 [http://www.msss.com/mars\\_images/moc/2005/09/20/dunegullies/](http://www.msss.com/mars_images/moc/2005/09/20/dunegullies/)), showing a new dune  
 1511 gully in Matara crater. Some additional detections were reported in refereed publications  
 1512 by Malin et al. (2006). A few candidate changes were suggested for HiRISE imaging by  
 1513 the Mars Reconnaissance Orbiter Context Camera team after being observed in their data;  
 1514 we thank them for calling them to our attention. Sara Martinez-Alonso and Virginia  
 1515 Gulick noted individual sites. Raack et al. (2015) discussed the activity in gullies at one  
 1516 south polar pit site in more detail than possible here.

1517 Supplementary Tables 1 and 2 are provided as separate CSV files. Supplementary  
 1518 Table 1 summarizes the following information for non-dune gullies (note that this  
 1519 includes gullies found in sandy material on non-dune steep slopes):

Field	Comment/Explanation
Site name	Geographic location and identifier number. Numbers index monitoring sites and therefore are non-sequential in this listing of active sites.
Latitude	Planetocentric
Longitude	East
Gully type	ACA indicates gullies with the classic alcove-channel-apron morphology. “Linear” gullies are generally sand-substrate gullies with small alcoves and long channels with little or no terminal deposit. “Channels” indicates gullies with minimal alcoves and aprons, but morphologically distinct from linear gullies.
Substrate	Non-sand, sand, light/rippled, or mixed. “Sand” refers to dark sand. “Light/rippled” refers to light-toned materials with ripples, suggesting aeolian modification, but lacking the dark blue color of active sand dunes on Mars (cf. Bridges et al., 2013). “Mixed” is used for cases where there is some component of dark sand within a gully that is mostly in non-sand material.

Orientation	Apparent downhill direction of the main slope. If flows of multiple orientations are summarized, the orientations are separated by semicolons.
Number of flows	Number of flows described by a given line. In some cases, individual events at a site have separate lines. In other cases, multiple similar events are reported together.
MY – before	Mars year of the last image before the change.*
L <sub>S</sub> – before	L <sub>S</sub> of the last image before the change.*
MY – after	Mars year of the last image before the change.*
L <sub>S</sub> – after	L <sub>S</sub> of the last image before the change.*
Bright?	Y if deposit is notably brighter than adjacent material in HiRISE red CCD, N otherwise.
Dark?	Y if deposit is notably darker than adjacent material in HiRISE red CCD, N otherwise.
Color?	States color if deposit is distinct in HiRISE color relative to adjacent material, N otherwise. U if there is no HiRISE color coverage. Colors are relative and based on color products with the near-IR/Red/Blue-green (IRB) filters assigned to red/green/blue channels, not true color.
Shadow-only?	Used for flows that appear distinct in a shadowed winter image, but are not visible when well-illuminated. Requires an “after” image with comparable shadows that does not show the flow in question.
Channel changes?	Y if there are visible changes in morphology along the channel for any of the flows, including brightness changes, deposition, and/or topographic changes of uncertain character. Includes cases of definite channel incision (next field).†
Channel incision?	Y if there is channel widening, deepening, extension, or formation of new channel segments, N otherwise.†
Thick deposit?	Y if there is a (near-)terminal deposit with visible thickness and topographic effects, N otherwise.†
Notes	Description of the changes, as needed. Coordinates of the form IMAGE_ID: X;Y give approximate locations of features of interest in HiRISE images. (These are from the red-filter RDR data product unless otherwise noted. They are typically chosen for good visibility of one of the more obvious parts of the change and are not necessarily the images that provide time constraints.) X and Y are pixel coordinates with the origin at upper left, with X increasing to the right and Y increasing downwards, as output by the HiView image viewer ( <a href="http://www.uahirise.org/hiview/">http://www.uahirise.org/hiview/</a> ).

1520 \*Image intervals are conservative. In some cases there are intervening images, but we  
1521 were not confident that it was possible to determine whether or not the change had  
1522 occurred in the image, typically because of poor lighting or seasonal frost cover.

1523 †Fields relating to topographic changes are U (uncertain) if there is no HiRISE image  
1524 before the event or an observation is marginal. They are L (Likely) if the images suggest  
1525 changes but the resolution/lighting match/scale of the changes is such that they are not  
1526 considered definite. Flows with no evidence for topographic change are marked N, but

1527 some of these may have changes that are not detectable in existing data. (For instance,  
1528 topography is difficult to see in high-Sun images.)

1529

1530           Supplementary Table 2 provides locations and brief descriptions of known active  
1531 dune gullies. Reiss et al. (2010) reported activity in the Russell crater linear gullies, and  
1532 Pasquon et al. (2016) documented activity at several linear gully sites. Due to the large  
1533 number of changes found in many dune gullies, the individual events are not listed  
1534 separately. Changes in minor alcove-apron features without defined channels occur on  
1535 many dunes but are not included here.

1536

1537

1538  
1539  
1540  
1541  
1542  
1543  
1544  
1545  
1546  
1547  
1548  
1549  
1550  
1551  
1552  
1553  
1554  
1555  
1556  
1557  
1558  
1559  
1560  
1561  
1562  
1563  
1564  
1565  
1566  
1567  
1568  
1569  
1570  
1571  
1572  
1573  
1574  
1575  
1576  
1577  
1578  
1579

## References

- Bridges, N. T., Geissler, P., Silvestro, S., Banks, M., 2013. Bedform migration on Mars: Current results and future plans. *Aeolian Research*, 9, 133-151, doi:10.1016/j.aeolia.2013.02.004. .
- Diniega, S., Byrne, S., Bridges, N.T., Dundas, C.M., McEwen, A.S., 2010. Seasonality of present-day Martian dune-gully activity. *Geology*, 38, 1047-1050, doi: 10.1130/G31287.1.
- Dundas, C.M., McEwen, A.S., Diniega, S., Byrne, S., Martinez-Alonso, S., 2010. New and recent gully activity on Mars as seen by HiRISE. *Geophys. Res. Lett.*, 37, L07202, doi: 10.1029/2009GL041351.
- Dundas, C.M., Diniega, S., Hansen, C.J., Byrne, S., McEwen, A.S., 2012. Seasonal activity and morphological changes in Martian gullies. *Icarus*, 220, 124-143, doi:10.1016/j.icarus.2012.04.005.
- Dundas, C.M., Diniega, S., McEwen, A.S., 2015. Long-term monitoring of Martian gully formation and evolution with MRO/HiRISE. *Icarus*, 251, 244-263, doi:10.1016/j.icarus.2014.05.013. .
- Hecht, M. H., 2002. Metastability of liquid water on Mars. *Icarus*, 156, 373-386, doi:10.1006/icar.2001.6794.
- Ingersoll, A. P., 1970. Mars: Occurrence of liquid water. *Science*, 168, 972-973.
- Landis, G.A., and the MER Athena Science Team, 2007. Observation of frost at the equator of Mars by the Opportunity rover. Lunar Planet. Sci. Conf. XXXVIII, abstract #2423.
- Malin, M.C., Edgett, K.S., Posiolova, L.V., McColley, S.M., Dobra, E.Z.N., 2006. Present-day impact cratering rate and contemporary gully activity on Mars. *Science*, 314, 1573–1577, doi: 10.1126/science.1135156.
- Pasquon, K., Gargani, J., Massé, M., Conway, S. J., 2016. Present-day formation and seasonal evolution of linear dune gullies on Mars. *Icarus*, 274, 195-210, doi:10.1016/j.icarus.2016.03.024.
- Piqueux, S., Kleinböhl, A., Hayne, P. O., Heavens, N. G., Kass, D. M., McCleese, D. J., Schofield, J. T., Shirley, J. H., 2016. Discovery of a widespread low-latitude diurnal CO<sub>2</sub> frost cycle on Mars. *J. Geophys. Res. Planets*, 121, doi:10.1002/2016JE005034.
- Raack, J., Reiss, D., Appéré, T., Vincendon, M., Ruesch, O., Hiesinger, H., 2015. Present-day seasonal gully activity in a south polar pit (Sisyphi Cavi) on Mars. *Icarus*, 251, doi:10.1016/j.icarus.2014.03.040.
- Reiss, D., Erkeling, G., Bauch, K.E., Hiesinger, H., 2010. Evidence for present day gully activity on the Russell crater dune field, Mars. *Geophys. Res. Lett.*, 37, L06203, doi: 10.1029/2009GL042192.
- Vincendon, M., Forget, F., Mustard, J., 2010a. Water ice at low to midlatitudes on Mars. *J. Geophys. Res.* 115, E10001, doi: 10.1029/2010JE003584.